frontiers | Frontiers in Marine Science

TYPE Original Research
PUBLISHED 21 April 2023
DOI 10.3389/fmars.2023.1122143

OPEN ACCESS

EDITED BY
Kostas Kiriakoulakis,
Liverpool John Moores University,
United Kingdom

REVIEWED BY
Yibo Liao,
Ministry of Natural Resources, China
Barbara Górska,
Institute of Oceanology (PAN), Poland
Mikołaj Mazurkiewicz,
Institute of Oceanology (PAN), Poland

*CORRESPONDENCE
Chih-Lin Wei
clwei@ntu.edu.tw

SPECIALTY SECTION
This article was submitted to Deep-Sea Environments and Ecology, a section of the journal Frontiers in Marine Science

RECEIVED 12 December 2022
ACCEPTED 28 March 2023
PUBLISHED 21 April 2023

CITATION
Tung C-C, Chen Y-T, Liao J-X and Wei C-L (2023) Response of the benthic biomass-size structure to a high-energy submarine canyon. *Front. Mar. Sci.* 10:1122143. doi: 10.3389/fmars.2023.1122143

Response of the benthic biomass-size structure to a high-energy submarine canyon

Chueh-Chen Tung[1], Yen-Ting Chen[1], Jian-Xiang Liao[1,2] and Chih-Lin Wei[1]*

[1]Institute of Oceanography, National Taiwan University, Taipei, Taiwan, [2]Taiwan Power Research Institute, Taiwan Power Company, Taipei, Taiwan

Introduction: Body size regulates all biological processes, including growth, reproduction, metabolism, trophic interactions, etc., and is the master trait across organisms, populations, and communities. Despite a rich literature on the impacts of human and natural disturbances on body size, a clear knowledge gap is the effect of the submarine canyons on the benthic size structures in the deep sea, hindering our understanding of the ecological processes of these dominant ecosystems on the continental margin.

Methods: Therefore, we conducted repeated sediment sampling to compare meiofauna and macrofauna biomass body-size spectrum, growth, metabolism, and size composition from a high-energy submarine canyon, Gaoping Submarine Canyon (GPSC), and the adjacent continental slope off SW Taiwan. The GPSC is a dynamic ecosystem connected to a high sediment-yield small mountain river subjected to strong internal-tide energy, swift bottom currents, frequent mass wasting events, and high terrestrial sediment inputs.

Results: We found that the meiofauna and macrofauna were characterized by relatively larger individuals dominating on the slope to smaller ones dominating in the canyon. As a result, the community biomass, secondary production, and respiration were depressed with distinctive biomass-size composition in the canyon compared to the non-canyon slope. The environmental factors related to internal tide disturbance (i.e., bottom current velocity, duration of sediment erosion, or low light transmission) substantially influence the body size composition of the canyon benthos, while food supplies (i.e., TOC and C/N ratio) and sediment characters (i.e., grain size and porosity) correlated closely with the slope communities.

Discussion: We concluded that the disturbed condition in the GPSC may have wiped out or depressed the local benthic assemblages, and only the smaller, more resilient species could persist. Our results also highlight that the alterations of the canyon benthic community could be a reference to deep-sea ecosystems under anthropogenic disturbances or global climate change.

KEYWORDS

meiobenthos, macrobenthos, submarine canyon, continental slope, biomass, biomass-size spectrum, secondary production, respiration

1 Introduction

Body size is a master trait affecting all biological processes and interactions among community groups (Elton, 1927; Kleiber, 1932), which is widely used to describe animal population, including growth, reproduction, and mortality (Pepin, 1991; Sukhotin et al., 2002; Moyano et al., 2017). Body size is also a key component of the metabolic theory of ecology (Peters, 1983; Brown et al., 2004) and directly influence metabolic rates, energy demands, and consumption rates of overall populations and communities (Klumpp, 1984; Vranken and Heip, 1986; Sommer et al., 1999). Therefore, animal density, respiration, and productivity in an ecosystem can be expressed through the allometric scaling of individual body size across taxa (Dickie et al., 1987; Boudreau and Dickie, 1989). Furthermore, body size affects energy and matter fluxes in marine sedimentary environments, especially for species that develop biogenic habitats (Norkko et al., 2013). While small individuals may dominate specific ecosystem functions due to their high abundance and rapid turnover, large-size individuals can modify habitats through bioturbations and bioirrigations, altering nutrient and organic matter cycling at the sediment-water interface (Aller, 1978; Volkenborn et al., 2012; Wrede et al., 2019).

In size-based ecosystem modeling, the biomass-size spectrum is the most widely used method to express the size structure of a community (Blanchard et al., 2017). The biomass-size spectrum refers to the distribution of living biomass across the organism size range of a community, estimating biomass in size categories that increase logarithmically and first applied to the planktonic community in the 1960s (Parsons, 1969; Sheldon et al., 1972; Platt, 1985). Usually, a linear relationship emerges when abundance and body mass are plotted on logarithmic scales. This suggests that the abundance is a power law function of body size, with many more small planktonic organisms than large ones. The dome patterns on the biomass size spectrum reveal how individual size governs feeding interactions and biological rates (Rossberg et al., 2019). The changes in body mass or abundance indicate trophic relationships. Changes in abundance and size can alter the slope of the spectrum, which in turn affects trophic interactions and carbon and nutrient cycling in the ecosystem (Petchey and Belgrano, 2010; Blanchard et al., 2017). Other than predator-prey interactions, anthropogenic activities can also affect the size structure. The exploited ecosystem usually has a steeper size-spectrum slope because fishery selectively targets large fish with a slow recovery rate and allows small fish to escape, resulting in a high abundance of small fish relative to large ones in the ecosystem (Shin et al., 2005). Other human-caused disturbances, such as habitat destruction, invasive species, and pollution, may have similar effects by steepening the slope of the biomass-size spectrum in the impacted ecosystems (Petchey and Belgrano, 2010).

The biomass-size spectrum has also been applied in the freshwater and benthic communities (Schwinghamer, 1981; Sprules et al., 1983; Sprules and Bowerman, 1988; Gaedke, 1992), suggesting that the physical environment may affect the communities by creating habitats for organisms of different size classes (Schwinghamer, 1981). The community with specific body size spectrums may carve a distinct niche by influencing the biological processes, including metabolism, respiration, movement, development, trophic interaction, and carbon flux (Sprules et al., 1991; Duplisea and Kerr, 1995; Blanchard et al., 2017). Thus, deviations in the size spectrum may be used to identify environmental impacts. Efforts have been devoted to detect responses of the benthic size spectrum to environmental conditions, such as the oxygen minimum zone (Quiroga et al., 2005), coastal hypoxia (Qu et al., 2015), seasonal input of organic matters (Soltwedel et al., 1996), and declining food supply with depth (Górska et al., 2020). However, some studies have found that the shapes of the size spectrum are not strongly affected by latitudinal temperature (Mazurkiewicz et al., 2020) and water depth variations (Schewe and Soltwedel, 1999).

In soft-sediment ecosystems, the responses to environmental disturbances vary with body sizes (i.e., macrofauna and meiofauna) and life history traits. Larger organisms have higher energetic requirements, slower growth, and lower reproductive output (Brey, 1999) making them more vulnerable to environmental disturbances (Giere, 2009). In addition, macrobenthos is considered more sensitive to physical disturbances (Austen and Widdicombe, 2006) and extinction risks (Solan et al., 2004). For example, in the Bilbao Estuary, Spain, the meiofauna biomass dominated over macrofauna along a pollution gradient (Saiz-Salinas and González-Oreja, 2000). Following the Deepwater Horizon (DWH) oil spill in the Gulf of Mexico, the macrofauna abundance was lowest within 3 km from the blowout site and then increased to the natural background conditions. In contrast, meiofauna abundance and the ratio of the nematode to copepod increased from the strong (< 3 km from the blowout site) to the moderate (17 km towards the southwest and 8.5 km towards the northeast from the blowout site) impacted area (Montagna et al., 2013). In the Arctic, glacial disturbances were reported to shift benthic biomass and production from macrofauna to meiofauna (Górska and Włodarska-Kowalczuk, 2017). Under climate change, organic carbon export and benthic biomass are projected to decline, and biomass loss is expected to be more rapid for macrofauna than for meiofauna (Jones et al., 2014). Despite significant efforts in studying biomass size spectra, to our knowledge, no study has yet to examine the effect of dominant geomorphological features, such as submarine canyons, on benthic-size structures in the deep sea, hindering the understanding of biological processes in the canyon ecosystem.

The seafloor consists of diverse habitats, and the submarine canyon is among the most prominent geological features on the continental margin. The variations in the origin, evolution, morphology, sediment transports and hydrodynamic regimes of canyons contribute to the heterogeneous distribution of benthic communities (Levin and Sibuet, 2012). Due to the organic accumulation in these topographic lows, the submarine canyons are usually hotspots of abundance and diversity (Vetter and Dayton, 1998; Vetter and Dayton, 1999; De Leo et al., 2010; Wei et al., 2012). However, in the southwest Taiwan continental margin, the Gaoping Submarine Canyon (GPSC) is connected to a small mountainous river (Chiang et al., 2020; Chiang and Yu, 2022). The extremely high sediment load, frequent turbidity currents, and strong internal tides within the river-fed GPSC result in a highly disturbed seabed

environment (Chiou et al., 2011; Lin et al., 2013; Liu et al., 2016), suppressing the abundance and diversity of the benthos (Liao et al., 2017; Liao et al., 2020). This study's principal objective was to use a size-based approach to examine community responses under intense disturbances in the submarine canyon. We used the high-energy GPSC as a test bed to compare with the adjacent continental slope at a similar depth. We predict that the biomass and body size of both meiofauna and macrofauna would decrease more rapidly in the disturbed canyons (Austen and Widdicombe, 2006). The changes in benthic size structure are expected to affect ecosystem functioning, including growth, respiration, and size composition, and ultimately the transfer of materials and energy in the food chain and sediment-water interface.

2 Materials and methods

2.1 Study area

GPSC is a major conduit of marine-terrestrial materials between the active Taiwan margin and the deep South China Sea. The deeply-incised canyon head cut into the continental shelf with a clear bathymetric connection to a small mountain river, the Gaoping River, with extremely high sediment loads (Chiang et al., 2020; Chiang and Yu, 2022). Therefore, the entire length of the GPSC is characterized by its meandering, V-shaped, and entrenched thalweg with deep-cutting outer bends (Figure 1). These erosive features are believed to be maintained by turbidity currents triggered by river flooding (Lin et al., 2013; Lin et al., 2016), internal tides (Wang et al., 2008; Lee et al., 2009; Chiou et al., 2011), groundwater discharges (Su et al., 2012), and sediment slumping (Hsu et al., 2008; Su et al., 2012; Gavey et al., 2017). The energy of internal tides is estimated to be 3–7 times greater than that in the well-known Monterey Canyon of similar shape and size (Lee et al., 2009), with a bottom current velocity ranging between 1.4-1.7 m/s and increasing toward the canyon head (Wang et al., 2008). The isothermal displacement by the internal tides can be over 200 meters (Liu et al., 2016), resulting in the benthic nepheloid layer as thick as 100 m with the suspended sediment concentration reaching 30 mg/l (Liu et al., 2010; Liao et al., 2017). The turbulence mixing by internal tides, high suspended-sediment concentrations near the seabed, and frequent turbidity currents suggest that the GPSC is a high-energy and disturbed ecosystem (Liu et al., 2016).

2.2 Sampling design

Four stations in the upper Gaoping Submarine Canyon (GC1 to GC4) and four stations on the adjacent slope (GS1 to GS4) were repeatedly sampled onboard R/V Ocean Researcher 1 (Figure 1; Table 1). The canyon and slope pairs were sampled by depth strata

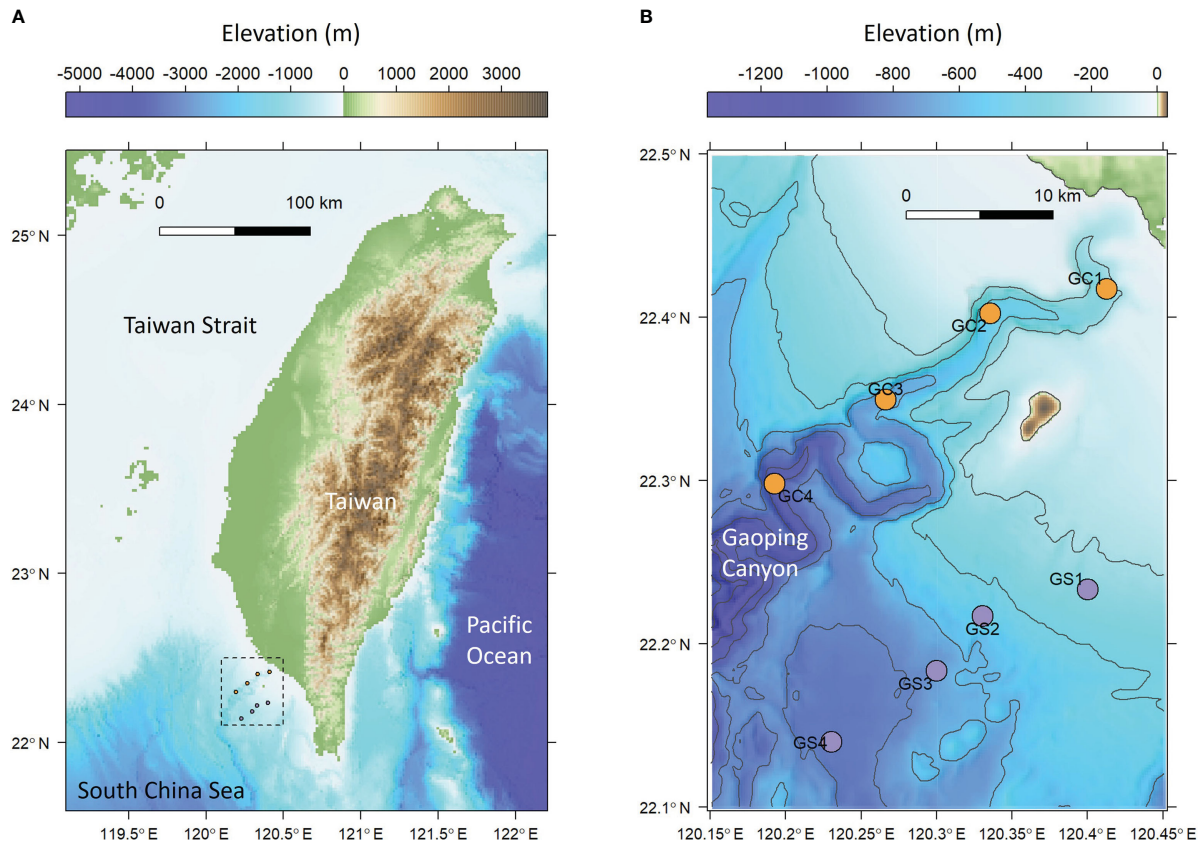

FIGURE 1
Sampling map of meiobenthos and macrobenthos. **(A)** The sampling area off the continental margin of SW Taiwan. **(B)** Sampling transects along the upper Gaoping Submarine Canyon (GC) and Gaoping Slope (GS).

10.3389/fmars.2023.1122143

TABLE 1 Sampling times and locations for boxcorer, multicorer, and CTD.

Habitat	Cruise	Station	Longitude	Latitude	Depth	Date
Canyon	1096	GC1	120.4170	22.4170	222	2014-11-28
		GC2	120.3418	22.4078	462	2014-11-26
		GC3	120.2664	22.3500	655	2014-11-27
	1102	GC1	120.4114	22.4173	323	2015-04-06
		GC2	120.3327	22.4004	482	2015-04-06
		GC3	120.2665	22.3483	653	2015-04-06
		GC4	120.1921	22.2981	1065	2015-04-06
	1114	GC1	120.4114	22.4172	320	2015-08-04
		GC2	120.3348	22.4007	478	2015-08-04
		GC3	120.2665	22.3501	655	2015-08-04
		GC4	120.1928	22.2980	1051	2015-08-05
	1126	GC1	120.4112	22.4175	318	2015-11-21
		GC2	120.3335	22.4003	487	2015-11-21
		GC3	120.2663	22.3492	655	2015-11-20
		GC4	120.1929	22.2982	1068	2015-11-20
Slope	1096	GS1	120.4006	22.2349	270	2014-11-27
		GS2	120.3332	22.2166	465	2014-11-28
		GS3	120.2997	22.1837	692	2014-11-28
	1102	GS1	120.4006	22.2329	279	2015-04-07
		GS2	120.3298	22.2168	464	2015-04-07
		GS3	120.3001	22.1831	682	2015-04-07
		GS4	120.2311	22.1392	840	2015-04-07
	1114	GS1	120.3998	22.2322	279	2015-08-05
		GS2	120.3297	22.2172	462	2015-08-05
		GS3	120.2998	22.1833	690	2015-08-05
		GS4	120.2304	22.1401	848	2015-08-05
	1126	GS1	120.3995	22.2329	277	2015-11-19
		GS2	120.3298	22.2167	463	2015-11-19
		GS3	120.3002	22.1829	690	2015-11-19
		GS4	120.2293	22.1400	848	2015-11-20

(200–400 m, 400–600 m, 600–800 m, and 800–1,100 m). The same stations were visited in November 2014 (OR1-1096), April 2015 (OR1-1102), August 2015 (OR1-1114), and November 2015 (OR1-1126). However, the OR1-1096 only sampled the first three depth strata (200–400 m, 400–600 m, and 600–800 m). We conducted a CTD cast and a boxcorer (November 2014 and April 2015) or multicorer (August 2015 and November 2015) at each station. For the boxcorer, five transparent polycarbonate tubes (i.d. = 67 mm) were inserted into the sample onboard to recover surface sediments. For the multicorer, twelve polycarbonate tubes (i.d. = 105 mm) can be retrieved from a single drop.

2.3 Biological sampling

During Aug 2015 and Nov 2015 cruises, one multicore tube (i.d. = 105 mm) per station was selected for meiofaunal analysis. We used a cut-off syringe (i.d., 28 mm; area 616 mm^2) to take three subsamples (top 5 cm of the sediment) from the recovered core tube; however, only one subsample was retrieved from the deepest canyon station (GC4) during Nov 2015 cruise. Altogether, 46 meiofauna subsamples were retrieved during the two cruises. On average, we selected three tubes from boxcorer (Nov 2014 and Apr 2015 cruises) or multicorer (Aug 2015 and Nov 2015 cruises) for macrofaunal analysis per station. The

top 15 cm of the sediments was extruded and washed with filter seawater (with a 5-μm filter) through a 300-μm sieve. In total, 100 macrofauna samples were retrieved during the four cruises. The sediment samples for meiofauna and macrofauna (after sieving) were fixed in the 5% formalin solution with Rose Bengal for at least one week. Boxcorer is known to create bow waves (Narayanaswamy et al., 2016), possibly resulting in sediment disturbance, loss of associated fauna (Bett et al., 1994), and underestimating macrofauna abundance (Montagna et al., 2017). Nevertheless, our macrofauna densities were comparable between the samples collected by boxcorer and multicorer (see Table A1 in Liao et al., 2017), suggesting that the gear effects are insignificant.

2.4 Body size measurements

The fixed meiofauna samples were washed with tap water through a 1000-μm sieve on top of a 40-μm sieve. The remaining sediments were immersed in Ludox HS40 solution (gravity = 1.18 g/cm^3), centrifuged at 8,000 rpm for 10 min, and repeated three times to extract meiofauna (Danovaro, 2010). After extraction, the fauna samples were transferred to 70% ethanol before sorting and counting under a stereo microscope (Olympus SZ61). From each meiofauna sample, only 100 nematode individuals (or all individuals if fewer than 100 were present) were randomly picked out and transferred to a solution of 5% glycerol and 5% ethanol in water. The mixture evaporated gradually on a warm hotplate, leaving the nematodes in pure glycerol. The nematodes were mounted onto permanent slides, and the length and width of the nematodes were measured by an ocular micrometer mounted on a compound microscope (Olympus BX53). The length and width of the remaining meiofauna and macrofauna specimens were measured by an ocular micrometer under a stereo microscope. We used ImageJ software to measure the macrofauna polychaete length and width from a photo by a camera mounted on a stereo microscope. Both the precisions of the ocular micrometer and image analysis are 1 μm.

The biovolumes of meiofauna and macrofauna specimens were calculated with the formula: $V = L \times W^2 \times C$, where V is the volume, L is the length, W is the width, and C is the taxon-specific conversion factors (Rachor, 1975; Warwick and Gee, 1984; Feller and Warwick, 1988). For the taxa whose conversion factors are unavailable, the biovolumes were calculated from length and width using the nearest geometric shapes (e.g., scaphopods - cone; aplacophorans - cylinder; sipunculans - cylinder; ophiuroids - ellipsoid or cylinder; asteroids - ellipsoid; nemerteans - cylinder). Finally, the biovolumes of meiofauna and macrofauna were converted into wet weight, assuming a specific gravity of 1.13 (Warwick and Gee, 1984).

2.5 Environmental condition

We measured the temperature (*Temp*), salinity (*Salin*), density (*Dens*), dissolved oxygen concentration (*O2*), fluorescence (*Fluo*), and light transmission (*Trans*) of the bottom water using a conductivity-temperature-depth (CTD) recorder (Sea-Bird SBE 911) and other attached sensors (Table 2). Surface sediment grain sizes (non-carbonate fraction), including percent clay, silt, and sand, were measured by a laser diffraction particle size analyzer (Beckman Coulter LS13 320). Total organic carbon (*TOC*) and total nitrogen (*TN*) were analyzed with a Flash EA 1112 elemental analyzer. TOC/TN calculated the C/N ratio. Porosity (*Por*) was estimated from the sediment's wet and dry weight, assuming a dry sediment density of 2.65 g/cm^3. Hourly bottom current velocity at each site was derived from a 3-D, hydrodynamic internal tide model from Chiou et al. (2011). Based on the internal tide model, we calculated the hourly mean velocity of bottom currents (*Spd*) and the duration for which bottom current speed exceeded 20 cm/s for one month preceding the sampling campaign (*Over20*) to estimate the disturbances of near-bottom currents.

We removed the redundant environmental variables (correlations > 0.9) before analyses. For example, the bottom water temperature, density, and dissolved oxygen measured were highly correlated; therefore, the dissolved oxygen (*O2*) was removed because the bottom water was well-oxygenated (O_2 > 2 mg/L), presumably, due to turbulence mixing by internal tides. The density (*Dens*) was removed because it's not known to affect infauna assemblages. We only retained bottom water temperature (*Temp*), salinity (*Salin*), light transmission (*Trans*), percent sand, silt, and clay, sediment TOC and C/N ratio, porosity (*Por*), and mean bottom current speed (*Spd*) and disturbance duration (*Over20*). These variables were logarithm (base of 10) transformed, centered (subtracted from the mean), and normalized (divided by the standard deviation) before use in statistical analyses involving environmental variables.

2.6 Data analysis

2.6.1 Biomass size spectrum

Because not all nematode specimens were measured for their sizes, the observed size measurements (from 100 random individuals) were randomly resampled (with replacement) to scale to the total nematode abundance. Polychaetes and ophiuroids are easy to break off. Therefore, we randomly resampled the measurements of complete specimens to the total abundance in a sample (e.g., polychaete with head and ophiuroids with disk). The individual sizes of meiofauna or macrofauna collected from the GPSC or adjacent slope (across all cruises and stations) were binned by $\log_2$ transformation of their biomass. The biomass within each size bin was $\log_{10}$ transformed and plotted against the $\log_{10}$ midpoint of the size bin to visualize the biomass size spectrum (BSS). For the normalized biomass size spectrum (NBSS), the total biomass of each size bin was divided by the width of the bin. The normalized biomass within each size bin was also $\log_{10}$-transformed and then plotted against the $\log_{10}$ midpoint of the size bin. The slope of the NBSS was estimated by fitting bounded power law (PLB) distribution to individual size distribution (ISD) using maximum likelihood estimation (MLE). The fitted line (with a 95% confidence interval) was plotted on the ISD, which ranks the body size in decreasing order to visualize the fit between the model and size data. The NBSS slope determined by MLE is equivalent to the regression slope of the NBSS; however, comparison studies by

10.3389/fmars.2023.1122143

TABLE 2 Environmental data collected along with the biological sampling.

Habitat	Cruise	Station	Temp	Dens	Salin	O2	Fluo	Trans	Clay	Silt	Sand	TOC	TN	CN	Por	Spd	Over20
			°C	kg m-3		mg L-1	µg L-1	%	%	%	%	%	%			m/s	%
Canyon	1096	GC1	15.5	1026.5	34.5	4.7	0.30	0.0	17.5	75.2	7.3	0.4	0.06	5.5	0.50	0.03	0.00
		GC2	8.5	1028.9	34.4	3.6	0.14	0.4	4.1	30.6	65.3	0.2	0.05	4.6	0.47	0.09	0.42
		GC3	9.0	1029.6	34.4	3.7	0.20	0.0	16.2	72.6	11.2	0.3	0.06	5.6	0.52	0.07	0.28
	1102	GC1	14.5	1027.1	34.5	4.6	0.06	21.6	10.0	45.6	44.4	0.3	0.05	5.5	0.42	0.10	6.53
		GC2	8.6	1028.9	34.4	3.6	0.05	32.6	1.1	6.4	92.4	0.2	0.05	4.6	0.27	0.09	6.53
		GC3	7.8	1029.8	34.4	3.5	0.04	43.3	12.7	53.8	33.5	0.4	0.06	6.2	0.45	0.09	0.83
		GC4	4.3	1032.2	34.5	3.2	0.02	66.8	21.7	76.5	1.8	0.6	0.09	6.1	0.55	0.08	1.25
	1114	GC1	13.2	1027.4	34.5	4.3	0.10	4.4	13.3	61.1	25.6	0.4	0.07	5.9	0.64	0.11	8.47
		GC2	8.6	1028.9	34.4	3.5	0.14	1.0	17.9	64.9	17.2	0.4	0.08	6.0	0.64	0.10	7.22
		GC3	8.0	1029.8	34.4	3.4	0.17	0.0	34.1	65.9	0.0	0.5	0.08	6.7	0.69	0.09	1.81
		GC4	4.0	1032.3	34.5	3.1	0.03	49.1	20.3	76.6	3.1	0.6	0.09	6.7	0.76	0.09	1.39
	1126	GC1	12.4	1027.5	34.5	4.4	0.07	19.2	21.0	77.2	1.8	0.4	0.08	5.8	0.61	0.11	4.17
		GC2	7.4	1029.1	34.4	3.5	0.02	42.5	4.7	54.5	40.8	0.3	0.05	5.5	0.54	0.10	7.50
		GC3	7.5	1029.6	34.4	3.5	0.03	61.2	22.3	76.5	1.2	0.4	0.08	5.4	0.74	0.09	1.39
		GC4	4.0	1032.3	34.5	3.2	0.03	51.2	23.6	75.5	0.9	0.6	0.10	5.7	0.78	0.07	0.14
Slope	1096	GS1	14.8	1026.8	34.6	5.0	0.02	84.5	21.2	75.6	3.2	0.5	0.09	5.5	0.59	0.06	0.00
		GS2	9.8	1028.5	34.4	4.0	0.03	75.3	22.7	75.7	1.6	0.6	0.11	5.6	0.64	0.07	0.00
		GS3	6.4	1030.2	34.4	3.2	0.02	87.3	26.4	73.1	0.5	0.6	0.11	5.5	0.64	0.05	0.00
	1102	GS1	14.2	1026.9	34.5	5.0	0.02	87.9	15.4	77.5	7.1	0.6	0.10	5.8	0.57	0.09	2.08
		GS2	9.5	1028.6	34.4	3.8	0.02	86.7	20.7	77.4	1.9	0.7	0.11	5.9	0.66	0.06	0.00
		GS3	7.2	1030.0	34.4	3.3	0.02	89.2	22.3	75.1	2.6	0.6	0.11	5.7	0.63	0.06	0.00
		GS4	5.9	1030.9	34.4	3.1	0.02	85.8	26.1	72.7	1.2	0.7	0.12	6.3	0.67	0.09	0.42
	1114	GS1	13.7	1027.1	34.5	4.6	0.03	76.9	12.6	78.1	9.3	0.5	0.08	6.2	0.67	0.08	1.81
		GS2	10.2	1028.5	34.4	3.9	0.02	87.3	19.8	77.5	2.7	0.7	0.11	6.2	0.78	0.06	0.14
		GS3	6.9	1030.1	34.4	3.2	0.02	86.5	24.3	74.0	1.7	0.8	0.12	6.2	0.77	0.05	0.00
		GS4	5.9	1031.0	34.4	3.0	0.02	83.6	22.4	75.9	1.7	0.8	0.12	6.7	0.84	0.08	0.00
	1126	GS1	13.9	1027.0	34.5	5.0	0.02	83.6	14.7	77.0	8.3	0.6	0.09	6.1	0.73	0.09	1.94
		GS2	9.0	1028.7	34.4	3.8	0.01	84.8	21.3	76.7	2.0	0.7	0.11	5.9	0.74	0.06	0.28
		GS3	6.4	1030.2	34.4	3.3	0.02	87.1	23.9	75.1	1.0	0.6	0.12	5.5	0.74	0.06	0.00
		GS4	5.5	1031.0	34.5	3.2	0.02	86.6	26.0	73.2	0.8	0.8	0.13	6.3	0.81	0.07	0.00

Edwards et al. (2017) concluded that the MLE method provides a better estimate of the NBSS slope.

2.6.2 Production and respiration

Meiofauna production to biomass ratio (P/B) was estimated using the following equation developed by Schwinghamer et al. (1986): $P/B = 0.073 \times M^{-0.337}$, where M is individual body mass [kcal]. We converted the macrofauna individual body mass (in mg wet weight) into energy content [J] using taxon-specific conversion factors from Brey (1999) (Excel table available from http://www.thomas-brey.de/science/DBconversion/datafiles/Conversion03.zip). We estimated macrofaunal annual production to biomass ratio (P/B) and secondary production (P) from three continuous parameters (temperature, water depth, body mass) and 17 categorical parameters (5 taxa, 7 lifestyles, 4 environments, and state of exploitation) using the Artificial Neural Network model (ANN) developed by Brey (2012) using R package BenthicPro (Andresen and Brey, 2018). The macrofauna-size nematode production to biomass ratio was estimated using the same equation from Schwinghamer et al. (1986). We multiplied the biomass of meiofauna and macrofauna with the annual P/B ratio to estimate secondary production.

Mass-specific respiration rates of meiofauna and macrofauna were estimated from body mass and temperature using an empirical

model, $\log_{10}(R/M) = 8.3732 - 0.2073 \times \log_{10}(M) - 2766.0235/T$, based on an extensive database compilated for aquatic invertebrate respiration (< 22000 measurements, > 900 species, > 440 references) by Thomas Brey (available from http://www.thomas-brey.de/science/virtualhandbook/respir/rempirics1.html). In the equation, R/M is the mass-specific respiration (J/J/day), M is individual body mass (J), and T is water temperature (K).

The annual secondary production and daily respiration rate were converted to units in wet weight, joule (J), and organic carbon weight using taxon-specific conversion from Brey (1999) (Tables S1, S2).

2.6.3 Size composition

The individual sizes of meiofauna and macrofauna were binned by the $\log_2$ transformation of their biomass. The total biomass of each size bin and each sample was then calculated as size composition for further multivariate analysis. The biomass in each $\log_2$ size bin and sample (i.e., core tube) was square-root transformed and converted to Bray-Curtis dissimilarity between samples. The same matrix was then subjected to Non-metric Multi-dimensional Scaling (nMDS). The mid-point of the $\log_2$ size bins was projected onto the nMDS plot by the biomass-weighted averages of the ordination scores within each size bin. Distance-based Redundancy Analysis (dbRDA) was used to model the size composition using environmental variables and select the subset of environmental variables which best explained (with the smallest AIC) the size composition. The selected variables were projected as vectors onto the same nMDS ordination, with the length of vectors indicating their correlations with the nMDS ordination scores and the direction of vectors indicating the direction of increasing environmental values.

2.6.4 Statistical test

We used Generalized Least Squares (GLS) modeling to examine the effects of habitat (canyon vs. slope), depth, and sampling time on the mean meiofauna and macrofauna biomass, production, P/B ratio, and respiration (by station). Also, three-way-cross permutation analysis of variance (PERMANOVA) was used to examine the effects of habitat, depth, and sampling time on the average meiofauna and macrofauna size composition. The number of permutations was set to 999. All statistical tests used α-value = 0.05, and pairwise tests used α-value = 0.05/numbers of trials (i.e., Bonferroni correction). All data analyses were conducted using software R version 4.2.1 (R Core Team, 2022). Normalized biomass size spectrum (NBSS), individual size distribution (ISD), and slope of NBSS were computed using R package *sizeSpectra* (Edwards et al., 2017). Multivariate analyses (i.e., nMDS, dbRDA, and PERMANOVA) used the R package *vegan*. Generalized Least Squares (GLS) modeling used the R package *nlme*. All relevant analyses can be reproduced from the R codes and data deposited in an R data package *bsss*, available at https://github.com/chihlinwei/bbbs.

3 Results

3.1 Environmental variations

Liao et al. (2017; Liao et al. 2020) analyzed the environmental data used in this study (Figure S1). Generally, they found that the modeled bottom current velocity (*Spd*) and duration of sediment erosion (*Over20*) increased in the canyon and toward the canyon head. The near-bottom light transmission and sediment *TOC* were lower in the canyon, and both were the lowest at the canyon head due to strong hydrodynamic energy. Furthermore, the bottom water temperature (*Temp*) and dissolved oxygen concentration (*O2*) declined with depth, but the surface *TOC* increased with depth along the canyon and slope transects.

3.2 Size structure

The individual size of meiofauna spanned from ca. 10^{-6} mg to over 1 mg wet weight (Figure 2A). Whereas the macrofauna size ranged from ca. 10^{-4} mg to over 100 mg wet weight. The largest meiofauna (> 0.1 mg) or macrofauna individuals (> 10 mg) occurred on the slope. The canyon meiofauna biomass peaks at mid-size bins (10^{-4} to 10^{-3} mg, Figure 2A), and the slope meiofauna appears to peak at size bins between 10^{-3} and 10^{-1} mg before the biomass dropped slightly and went back up again. Similarly, the biomass of the canyon macrofauna peaked at size bins between 10^{-2} and 10^{-1} mg before the biomass dropped slightly and then went back up again with increasing size bins. For both the meiofauna and macrofauna, the larger size bins contributed the most to the biomass difference between the canyon (orange symbols) and slope communities (purple symbols), and the canyon biomass was consistently lower than the slope biomass (Figure 2A).

The meiofauna and macrofauna NBSS are "dome" shapes, indicating low relative abundance for the smallest and the largest sizes (Figure 2B). When comparing the NBSS of meiofauna between the canyon and slope, a considerable amount of large-size individuals was lost in the canyon. For macrofauna, the relative abundance of the largest and smallest size classes decreased due to the "canyon" effect; however, more individuals were removed from the largest size bins than from the smallest size bins.

For the meiofauna size > 0.001 mg and macrofauna > 0.01 mg, the $\log_{10}$ normalized biomass declined linearly with the $\log_{10}$ mid-point of size bins. The decline of $\log_{10}$ normalized biomass with $\log_{10}$ mid-point of size bins (i.e., NBSS slope, Figure 2C) was more rapid for the canyon (i.e., regression slope = -2.51 and -2.07 for meiofauna and macrofauna, respectively) than for the slope assemblages (i.e., regression slope = -1.99 and -1.56 for meiofauna and macrofauna, respectively), indicating the relative abundance of largest size classes declined as we moved from the slope into the canyon. However, the NBSS slope of the canyon macrofauna was similar to that of the slope meiofauna. The NBSS slopes were

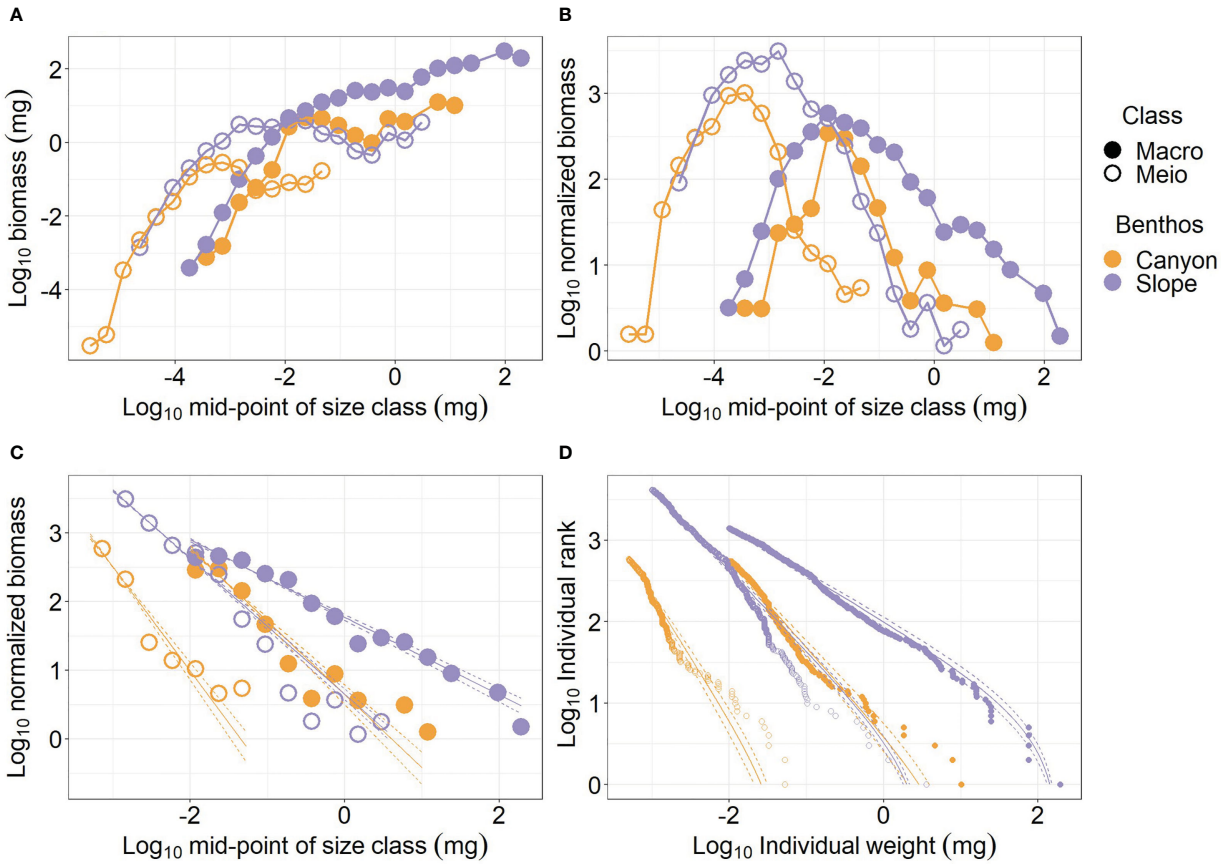

FIGURE 2
Size spectra of meiobenthos and macrobenthos. **(A)** biomass size spectrum (BSS); **(B)** normalized biomass size spectrum (NBSS); **(C)** NBSS excluding small size classes (i.e., meiofauna < 0.001 mg; macrofauna< 0.01 mg) **(D)** Individual sizes distribution (ISD) for panel **(C)**.

estimated from Individual sizes distribution (ISD). Figure 2D shows that the ISDs of the larger meiofauna and macrofauna fitted nicely to bounded power law distributions (PLB). When the size spectra of meiobenthos and macrobenthos are estimated by habitats and cruises (Figure S2), the general patterns are still similar to Figure 2. The NBSS slopes were steeper for larger meiofauna and macrofauna in the canyon. However, the ISDs by habitats and cruises (Figure S2D) did not fit bounded power law distributions (PLB) as well as the ISDs by habitats (Figure 2D).

The meiofauna body size measurements for each subcore (i.d. = 28 mm) were randomly resampled (with replacement) to scale to the coring area of a single multicore tube (i.d. = 105 mm) to examine the effect of different core sizes. Based on the simulated data, a multi-panel figure similar to Figure 2 was presented as Figure S3. Except for a much greater difference in NBSS elevations between the meiofauna and macrofauna, the general patterns (i.e., described in the above paragraph) are similar between the original (Figure 2) and the scaled biomass-size spectra (Figure S3). When the resampled meiofauna merged with the macrofauna size measurements (Figure S4), similar patterns, such as greater biomass on the slope (Figure S4A), "dome" shape NBSS peak ~ 10^{-3} mg (Figure S4B), and steeper NBSS slope in the canyon (Figure S4C), were observed between the merged and separated size spectra (Figure 2).

3.3 Biomass (wet weight)

Average meiofauna biomass on the slope (1,954.5 mg m^{-2}) was more than ten-folds and thus significantly higher than that in the canyon (92.1 mg m^{-2}, Table S1; Figure 3A) (Habitat, $P < 0.001$, Table 3). Despite that macrofaunal biomass appears to increase with depth in the canyon (albeit marginally, $P = 0.06$, Figure 3B), the average biomass on the slope was still nearly ten-fold (3,075 mg m^{-2}, Table S2) and significantly higher than that in the canyon (Habitat, $P < 0.001$, 328 mg m^{-2}, Table 4). On average, the macrofauna contributed 78.1% of the biomass in the canyon but 61.1% of biomass on the slope. Pairwise tests across four depth strata revealed significant habitat effects at depths from 200 to 400 m and from 400 to 600 m ($P < 0.01$) but not at depths from 600 to 800 m and 800 to 1100 m ($P > 0.1$). This discrepancy may have contributed to the significant interaction between habitat and depth in the main test (Habitat: Depth, $P = 0.024$, Table 4).

3.4 Production

The average P/B ratio of meiofauna in the canyon (ca. 9.5 yr^{-1}) was almost two times higher than that on the slope (ca. 4.5 yr^{-1}, Figure 4A; Table S1) (Habitat, $P = 0.04$, Table 3). The macrofaunal

10.3389/fmars.2023.1122143

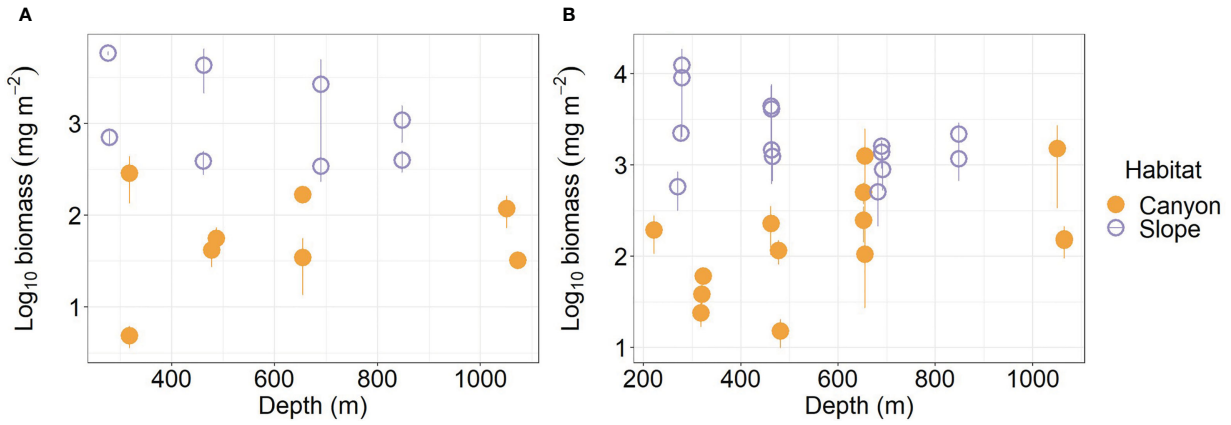

FIGURE 3
Biomass of meiobenthos **(A)** and macrobenthos **(B)** as functions of depth. Error bar shows standard deviation.

TABLE 3 ANOVA table of generalized least square (GLS) modeling on biomass, P/B ratio, production, mess-specific respiration, and respiration of meiofauna, as well as PERMANOVA table on size composition of meiofauna.

	DF	F-value	p-value		DF	F-value	p-value
Biomass				Mass-specific respiration			
(Intercept)	1	363.02	**0.000**	(Intercept)	1	148.09	**0.000**
Habitat	1	27.76	**0.001**	Habitat	1	6.67	**0.030**
Depth	1	0.08	0.780	Depth	1	10.45	**0.010**
Cruise	1	1.25	0.275	Cruise	1	0.19	0.672
Habitat : Depth	1	1.11	0.334	Habitat : Depth	1	0.64	0.445
Habitat : Cruise	1	3.09	0.107	Habitat : Cruise	1	0.64	0.446
Depth : Cruise	1	0.46	0.537	Depth : Cruise	1	0.34	0.573
P/B ratio				Respiration			
(Intercept)	1	119.19	**0.000**	(Intercept)	1	209.27	**0.000**
Habitat	1	15.14	**0.004**	Habitat	1	50.81	**0.000**
Depth	1	0.24	0.639	Depth	1	6.25	**0.034**
Cruise	1	0.90	0.368	Cruise	1	9.60	**0.013**
Habitat : Depth	1	0.95	0.354	Habitat : Depth	1	3.72	0.086
Habitat : Cruise	1	0.99	0.347	Habitat : Cruise	1	6.17	**0.035**
Depth : Cruise	1	1.17	0.307	Depth : Cruise	1	1.19	0.304
Production				Size composition			
(Intercept)	1	4532.57	**0.000**				
Habitat	1	57.70	**0.000**	Habitat	1	3.91	**0.001**
Depth	1	0.86	0.379	Depth	1	1.81	0.073
Cruise	1	14.86	**0.004**	Cruise	1	0.66	0.766
Habitat : Depth	1	3.94	0.078	Habitat : Depth	1	1.31	0.248
Habitat : Cruise	1	15.16	**0.004**	Habitat : Cruise	1	0.81	0.580
Depth : Cruise	1	2.26	0.167	Depth : Cruise	1	1.61	0.125

Bold fonts indicate $P < 0.05$.

10.3389/fmars.2023.1122143

TABLE 4 ANOVA table of generalized least square (GLS) modeling on biomass, P/B ratio, production, mess-specific respiration, and respiration of macrofauna, as well as PERMANOVA table on size composition of macrofauna.

	DF	F-value	p-value		DF	F-value	p-value
Biomass				Mass-specific respiration			
(Intercept)	1	919.95	**0.000**	(Intercept)	1	1603.65	**0.000**
Habitat	1	38.79	**0.000**	Habitat	1	0.03	0.866
Depth	1	0.95	0.346	Depth	1	109.33	**0.000**
Cruise	3	0.51	0.682	Cruise	3	1.22	0.337
Habitat : Depth	1	6.29	**0.024**	Habitat : Depth	1	3.90	0.067
Habitat : Cruise	3	1.29	0.315	Habitat : Cruise	3	0.35	0.793
Depth : Cruise	3	0.49	0.691	Depth : Cruise	3	0.09	0.962
P/B ratio				Respiration			
(Intercept)	1	2955.34	**0.000**	(Intercept)	1	123.17	**0.000**
Habitat	1	21.62	**0.000**	Habitat	1	14.81	**0.002**
Depth	1	97.97	**0.000**	Depth	1	5.98	**0.027**
Cruise	3	0.51	0.680	Cruise	3	0.95	0.444
Habitat : Depth	1	2.82	0.114	Habitat : Depth	1	8.33	**0.011**
Habitat : Cruise	3	0.79	0.516	Habitat : Cruise	3	2.39	0.110
Depth : Cruise	3	0.94	0.446	Depth : Cruise	3	1.18	0.352
Production				Size composition			
(Intercept)	1	1878.58	**0.000**				
Habitat	1	15.68	**0.001**	Habitat	1	4.06	**0.003**
Depth	1	3.26	0.091	Depth	1	1.95	0.064
Cruise	3	0.72	0.555	Cruise	3	1.55	0.087
Habitat : Depth	1	6.86	**0.019**	Habitat : Depth	1	0.78	0.635
Habitat : Cruise	3	2.04	0.151	Habitat : Cruise	3	0.87	0.644
Depth : Cruise	3	1.16	0.359	Depth : Cruise	3	1.53	0.076

Bold fonts indicate $P < 0.05$.

P/B ratio declined with depth in both habitats ($P < 0.01$, Figure 4B), but the P/B ratio of the slope assemblage was significantly higher than the canyon assemblage ($P < 0.001$, Table 4).

The average production of meiofauna was 28.4 mg C m^{-2} yr^{-1} in the canyon and 97.8 mg C m^{-2} yr^{-1} on the slope (Table S1). The average macrofauna production was 25 mg C m^{-2} yr^{-1} in the canyon and 72 mg C m^{-2} yr^{-1} on the slope (Table S2). The macrofauna, on average, contributed 47.1% of production in the canyon and 42.5% on the slope. As a result, the meiofaunal and macrofaunal productions were significantly higher on the slope than in the canyon (Production, $P < 0.01$, Tables 3, 4). The secondary production of both meiofauna and macrofauna declined with depth on the slope ($P < 0.05$) but not in the canyon (Figures 4C, D). Nevertheless, significant cruise effect and interaction between habitat and cruise were evident for meiofauna ($P = 0.04$, Table 3). Pairwise tests for meiofauna suggested that the cruise effect was only significant in the canyon (pairwise GLS, $P = 0.013$), and the habitat effect was only significant during Nov 2015 cruise (pairwise GLS, $P = 0.01$). Similarly, macrofauna showed a significant interaction between habitat and depth (Table 4). Pairwise tests suggested that the habitat effect was only marginally significant at depths from 200 to 400 m for macrofauna (pairwise GLS, $P = 0.02$, α-value = 0.05/4).

3.5 Respiration

Mass-specific respiration rate (R/M) for meiofauna declined significantly with depth in the canyon ($P < 0.001$), but the decline was only marginally significant with depth on the slope ($P = 0.05$, Figure 5A). In contrast, the R/M ratio for macrofauna declined significantly with depth in both canyon and slope ($P < 0.001$, Figure 5B). The R/M ratio of canyon meiofauna was significantly higher than that of the slope assemblages (Habitat, $P = 0.03$, Table 3); however, no statistical evidence suggests that the macrofaunal R/M ratio was different between the canyon and slope (Habitat, $P = 0.86$, Table 4).

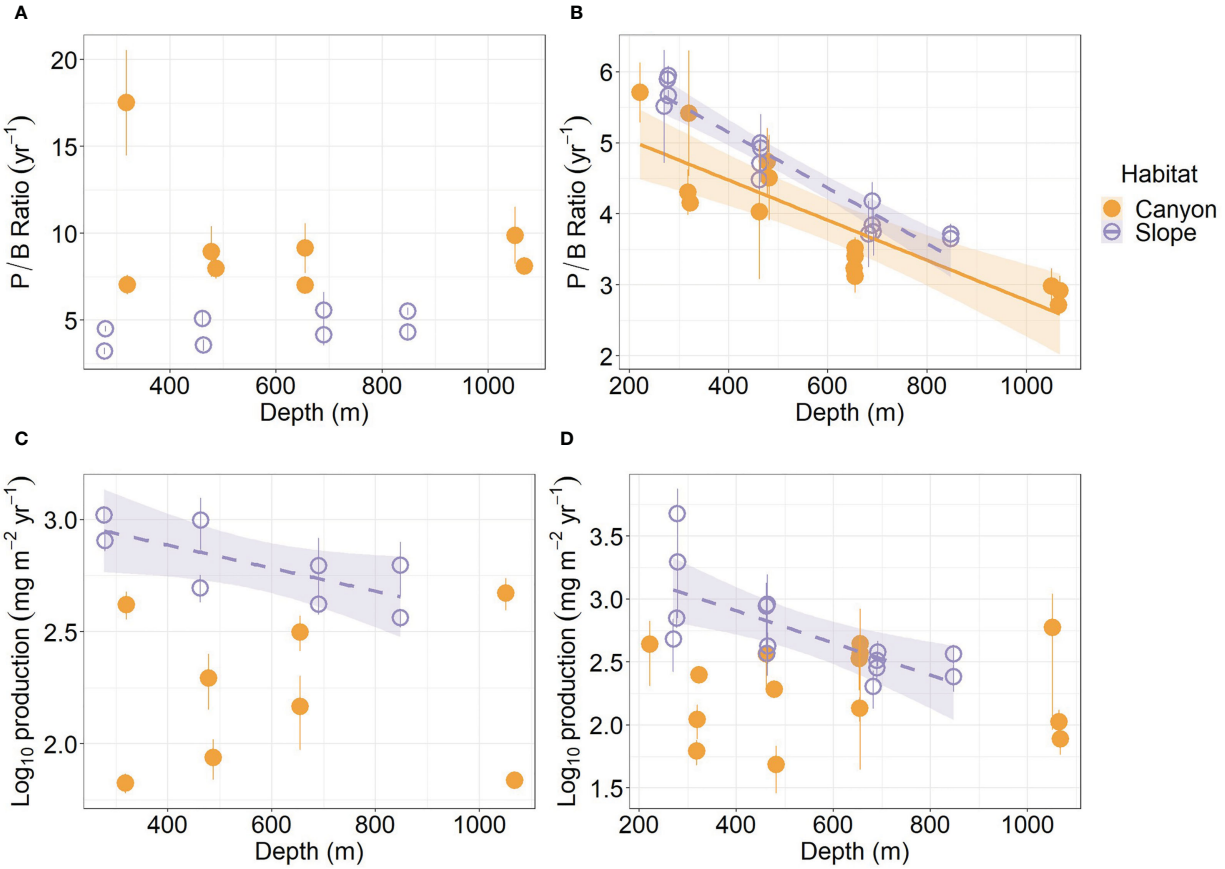

FIGURE 4
Annual P/B ratio and secondary production of meiobenthos **(A–C)** and macrobenthos **(B–D)** as functions of depth. Trend lines show significant relationships with depth based on simple linear regressions (P < 0.05), and shaded areas show 95% confidence intervals. Error bar indicates standard deviation.

The average respiration of meiofauna was 175.8 mg C m^{-2} yr^{-1} in the canyon and 841.7 mg C m^{-2} yr^{-1} on the slope (Table S1). In contrast, the average respiration of macrofauna was 113.8 mg C m^{-2} yr^{-1} in the canyon and 355.3 mg C m^{-2} yr^{-1} on the slope (Table S2). The macrofauna, on average, contributed 39.3% of respiration in the canyon and 29.7% of respiration on the slope. Meiofaunal and macrofaunal respiration declined significantly with depth on the slope (P < 0.02, Figures 5C, D). ANOVA (on GLS) suggests that the meiofaunal and macrofaunal respirations on the slope were significantly higher than that in the canyon (Habitat, P < 0.01, Tables 3, 4); however, there were also interactions between habitat and cruise for meiofauna (Habitat: Cruise, P = 0.04, Table 3) and habitat and depth for macrofauna (Habitat: Depth, P = 0.011, Table 4). For meiofauna, pairwise tests suggest that the habitat effect was only marginal during the August 2015 cruise (P = 0.03, α-value = 0.05/2) but was significant during the November 2015 cruise (P < 0.01). The cruise effect was only significant in the canyon (P = 0.02, α-value = 0.05/2). For macrofauna, pairwise tests suggest that the habitat effect was only marginal at depths between 200 to 400 m (P = 0.02, α-value = 0.05/4).

3.6 Size composition

Habitats were well-separated in the nMDS ordination of meiofaunal size composition (Figures 6A, B). In contrast, the ordination of macrofaunal size composition partly overlapped between the canyon and slope (Figures 6C, D). By projecting the midpoint of the size bins on the nMDS plots, the meiofaunal size bins appear progressively larger from the canyon to the slope (Figure 6A). In contrast, the macrofaunal size bins were clustered around the slope ordinations (Figure 6C), presumably, due to much higher biomass within each size bin on the slope than in the canyon (Figure 2A). Nevertheless, we can still see a clear size transition within the slope ordination for macrofauna (Figure 6C), in which the smaller size bins were closer to the canyon ordination (to the left) and larger size bins away from it (to the right).

The separation of nMDS ordination (whether distinct or partly) was also reflected by a significant between-habitat difference in meiofauna (Habitat, P = 0.001, Table 3) and macrofauna size composition (Habitat, P = 0.002, Table 4) in the PERMANOVA tests. In the meantime, only marginal depth effects were detected for

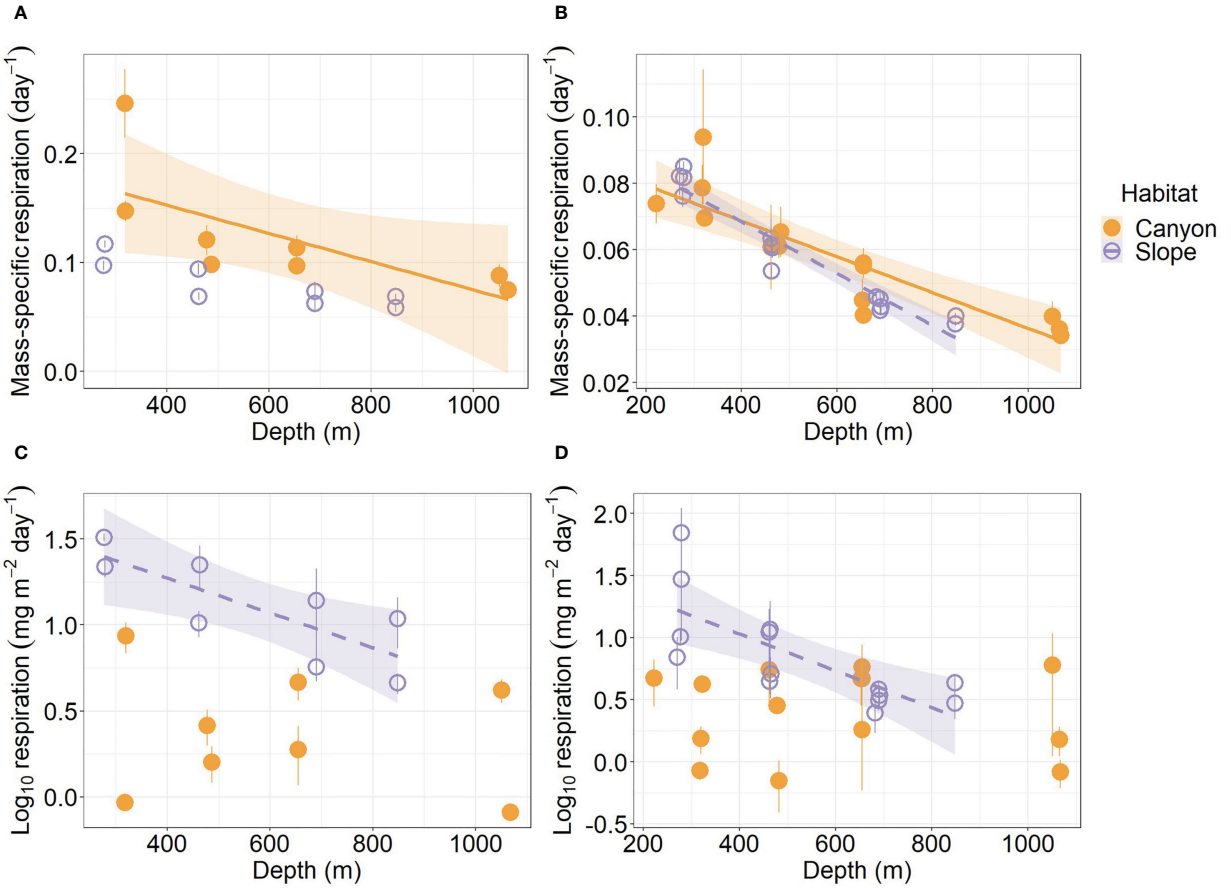

FIGURE 5
Mass-specific respiration and total respiration rate of meiobenthos **(A–C)** and macrobenthos **(B–D)** as functions of depth. Trend lines show significant relationships with depth based on simple linear regressions (P < 0.05), and shaded areas show 95% confidence intervals. The relationship between meiofaunal mass-specific respiration and depth was borderline significant on the slope (P = 0.05); thus, the trend line was not presented. Error bar shows standard deviation.

meiofaunal (Depth, P = 0.073, Table 3) and macrofaunal size composition (Depth, P = 0.064, Table 4).

Based on distance-based redundancy analysis (dbRDA), the best subset of environmental factors explaining meiofauna size composition (adjusted R^2 = 48.1%, p < 0.05) were variables related to 1) internal-tide energy, i.e., *Over20*; 2) food supply, i.e., *TOC*; 3) water masses, i.e., *Temp*; 4) sediment characteristics, i.e., *Silt*, *Clay* and *Por*. These variables are mapped onto the same nMDS plot (Figure 6B) using their correlations with the ordination axes, showing that the canyon assemblages were characterized by increasing *Over20* and the slope assemblages by increasing *TOC*, *Temp*, *Silt*, *Clay*, and *Por*.

For the macrofauna, the best subset of environmental factors explaining the size composition (adjusted R^2 = 27.7%, p < 0.05) were variables related to 1) Internal-tide energy, i.e., *Spd*, *Over20*, and *Trans*; 2) food supply, i.e., *CN*; 3) water masses, i.e., *Temp*; 4) sediment characteristics, i.e., *Por* and *Silt*. These variables are also mapped onto the nMDS plot (Figure 6D), showing that the canyon assemblages were characterized by increasing *Spd* and *Over20* and the slope assemblages by increasing *CN*, *Trans*, *Por*, and *Silt*.

4 Discussion

The localized maximums in normalized biomass size spectra (NBSS), also known as the "dome" patterns, are often observed in the aquatic ecosystem (Boudreau et al., 1991; Quiroga et al., 2014), especially in the pelagic communities (Rossberg et al., 2019). The cause of these "domes" is subject to debate, but the most common explanation is that these "domes" represent the trophic positions on the food chain or different taxonomic groups (Thompson et al., 2013; Kwong and Pakhomov, 2021). The subsequent domes on the NBSS may represent the size ratios between the predator and prey (Yurista et al., 2014; Atkinson et al., 2021). A recent study using a model and empirical data demonstrated that the "dome" patterns in NBSS might be driven by trophic cascade and nutrient availability (Rossberg et al., 2019). In theory, the trophic cascade (or predation) may modulate the community biomass toward the smaller classes, whereas the nutrient enrichment likely increases the density of the larger classes. The interaction between top-down trophic cascade and bottom-up nutrient enrichment is possible to generate the "dome" and "trough" in the NBSS for the theoretical model, which

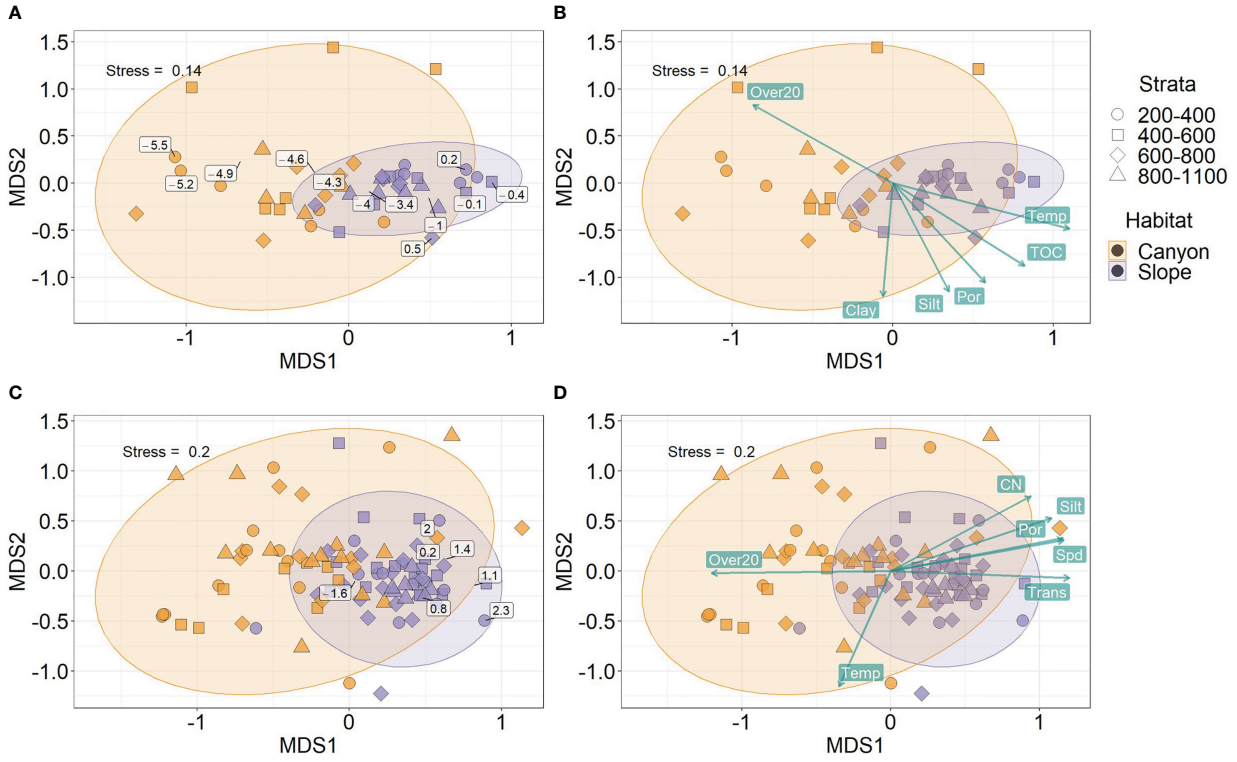

FIGURE 6
Non-metric Multi-dimensional Scaling (nMDS) on body size compositions of meiobenthos **(A, B)** and macrobenthos **(C, D)**. The biomass in each $\log_2$ size bin and sample was square-root transformed and converted to Bray-Curtis dissimilarity between samples before subjecting to nMDS. The text labels on panels **(A–C)** show the mid-point of the $\log_2$ size bins based on the biomass-weighted averages of the ordination scores within each size bin. The text labels on panels **(B–D)** show the best subset of environmental variables selected by Distance-based Redundancy Analysis (dbRDA). The length of vectors on panels **(B–D)** indicates environmental correlations with the nMDS ordination scores. The direction of vectors suggests increasing bottom water temperature (Temp), light transmission (Trans), percent silt and clay, sediment TOC and C/N ratio, porosity (Por), and mean bottom current speed (Spd) and disturbance duration (Over20).

has been validated by the empirical data (Rossberg et al., 2019). Interestingly, our study also observed distinct meiofauna and macrofauna "domes" in the NBSS, supporting the assertion by Rossberg et al. (2019) and others (Thompson et al., 2013; Yurista et al., 2014; Atkinson et al., 2021; Kwong and Pakhomov, 2021) on the trophic origin of the NBSS domes. Moreover, many manipulative and field experiments have confirmed meiofauna as an essential food source for higher trophic levels, including macrofauna (Coull, 1990; Ólafsson, 2003; Schratzberger and Ingels, 2018). Therefore, the trophic interactions between meiobenthos and macrobenthos can potentially result in two NBSS "domes" aligning in a step fashion along a linear trend.

However, the benthic community size structure is known to be less pronounced than the pelagic communities (Shurin et al., 2006). Therefore, to our knowledge, only a handful of benthic studies reported "dome" patterns in their NBSS. For instance, Quiroga et al. (2014) showed "dome" patterns in the NBSS for the Antarctic macrobenthic communities. Mazurkiewicz et al. (2019; Mazurkiewicz et al. 2020) reported consecutive "domes" in the NBSS for the Arctic fjord meiobenthos and macrobenthos, respectively. The bimodal size spectra suggest that meiofauna and macrofauna may be discrete entities (Schwinghamer, 1981; Warwick and Clarke, 1984; Warwick, 2014). Nevertheless, the "dome" patterns reported by these studies were less pronounced than those observed in our study. We did not expect sharp NBSS dips for meiofauna and macrofauna in their smallest and largest sizes, respectively (Figure 2B), because the infauna communities usually have flexible feeding strategies. For example, nearly all benthic carnivores are scavengers (Ruxton and Houston, 2004). Some polychaetes (i.e., *Nereis diversicolor*) can switch among deposit-feeding, scavenging, predation, or suspension-feeding, depending on the flow regimes (Biles et al., 2003). While unintentionally, the deposit-feeding macrofauna may consume meiofauna living in interstitial sediment spaces (Iken et al., 2001; Jumars et al., 2015). Liao et al. (2017; Liao et al. 2020) also examined the feeding strategies of polychaete and nematode specimens from this study. They found the polychaete feeding modes ranging from deposit feeders, carnivores, scavengers, omnivores, and suspension feeders, and nematodes from deposit feeders, epigrowth feeders, and omnivores/predators. Given the flexible feeding guilds of the meiobenthos and macrobenthos, it is likely that trophic cascade (or predation) may not be the only cause of our distinct "dome" patterns in the benthic NBSS.

Using mathematical simulation, Bett (2013) offers an alternative explanation for the "dome" patterns. He showed that the two "domes" and a "trough" in the biomass-size spectra could arise from a continuous size distribution with two hypothetic sieves. In other words, the sampling protocols or sieving artifacts can

contribute to the bimodal biomass-size spectra. Moreover, if we assume that all organisms are perfect spheres. The 40-μm sieve should retain meiofauna larger than 3 x 10^{-4} mg, and the 300-μm sieve should retain macrofauna larger than 1.6 x 10^{-2} mg. These thresholds are close to our cut-off sizes of 0.001 and 0.01 mg (see results for details) to generate linear NBSS for the larger meiobenthos and macrobenthos, respectively. Since most meiobenthos and macrobenthos are not spherical, the sieves might retain even smaller organisms. The retaining sediments can also clog the sieves, keeping the specimens that are supposed to pass the sieves. Still, the numbers of the inadvertently included organisms should decrease with decreasing body size, resulting in the left tail of the "dome" patterns. Nevertheless, it is impossible to determine the relative contributions of trophic position and sieving artifact to the "domes" and "troughs" of our observed NBSS.

We observed linear and negative NBSSs for meiofaunal (> 40 μm) and macrofaunal-size individuals (> 300 μm). Lower intercept and steeper slope of the NBSS were observed in the canyon habitat resulting in lower biomass of the meiofaunal and macrofaunal size individuals. It also means that the "canyon" conditions removed larger individuals with the effect increased toward the larger size classes. Similar patterns (i.e., steeper NBSS slope) have been observed in benthic communities from the coastal hypoxic zone in the Gulf of Mexico (Qu et al., 2015), oxygen minimum zones off Chile (Quiroga et al., 2005), and the Antarctic continental slope (Saiz-Salinas and Ramos, 1999). These studies suggest that the low oxygen conditions and food limitations may impact large organisms more than small ones. Small organisms can better satisfy their metabolic demands (i.e., oxygen demand or nutritional need) due to the relatively large surface area to body volume ratio. Under extreme hypoxia (DO < 1 mg/L), even the small species may decline in abundance, leading to the dominance of medium-sized species (Qu et al., 2015). However, this might not be the case in this study because the medium-size individuals dominated (i.e., dome patterns in Figure 2B) both the disturbed (i.e., canyon) and non-disturbed habitat (i.e., adjacent slope). Other studies using different statistical approaches (i.e., non-NBSS) also report an increasing abundance of smaller individuals (or shift biomass maximum to smaller size classes) due to habitat degradation and fishing (Wilson et al., 2010), glacial sedimentation (Górska and Włodarska-Kowalczuk, 2017), trawling disturbance (Queirós et al., 2006), and pollution (Hargrave and Thiel, 1983; Schwinghamer, 1988; Saiz-Salinas and González-Oreja, 2000). This study demonstrates that the responses of benthic communities to natural disturbances in GPSC may be as strong as the studies mentioned above. We also provide the first evidence for steepening NBSS slopes in a high-energy submarine canyon, suggesting that the physical conditions may be unfavorable for the local infauna communities.

Benthic biomass and production often decline with intensive bottom trawling (Jennings et al., 2001; Duplisea et al., 2002; Queirós et al., 2006), glacial disturbance (Górska and Włodarska-Kowalczuk, 2017), food limitation (Wei et al., 2010a), oxygen deficiency (Diaz and Rosenberg, 1995; Diaz and Rosenberg, 2001; Levin, 2003), and organic pollution (Hargrave and Thiel, 1983; Montagna et al., 2013). We observed similar depressed benthic biomass, production, and respiration in the canyon compared to the adjacent slope. Due to their larger size, macrofauna accounted for more benthic biomass than meiofauna. They contributed even more biomass in the GPSC (~78%) than on the adjacent slope (~61%). The GPSC experiences strong internal tide disturbance and thus was dominated by burrowing, motile, subsurface deposit-feeding polychaetes (i.e., paraonids, capitellids, and cosurrids) (Liao et al., 2017). These specialized animals can burrow deep into the sediments to feed on the organic particles while avoiding being swept away by strong bottom currents. Therefore, the higher contribution by macrofauna biomass in the GPSC could result from adapting life history traits to its unique environmental condition. The body size compositions in the canyon also differed from the non-canyon habitats, indicating that the energetic GPSC not only impacted the body size structure (i.e., steeper NBSS) but also the growth and metabolism of populations and communities (Brey, 1999; Sukhotin et al., 2002; Moyano et al., 2017). Likewise, our results were consistent with the previous studies, showing lower abundance, species diversity, functional diversity, and distinctive species composition in the GPSC compared to the adjacent slope habitat (Liao et al., 2017; Liao et al., 2020). Together, the multifaceted characteristics of community structure from this and previous studies suggest that GPSC is a high-energy and disturbed environment for the local benthic communities.

Interestingly, the canyon meiofauna had higher P/B ratios and mass-specific respiration rates than the slope meiofauna, suggesting that the r-strategists likely dominated the canyon meiofauna community with faster growth and high metabolic rates. This result is in accord with analyses based on nematode buccal and tail morphology and life-history strategies (Liao et al., 2020), in which the non-selective deposit feeders with clavate tail and r-selection strategy dominated the upper GPSC. Nevertheless, the extremely low meiofauna biomass in the canyon (i.e., more than ten folds lower) still resulted in lower meiofauna production and respiration than on the slope. In contrast with the higher meiofauna P/B ratios, the macrofauna P/B ratios were lower in the canyon than on the slope. The contradiction indicates that the extreme condition in the GPSC may negatively affect the macrofauna more than the meiofauna P/B ratios. Given the lower P/B ratio and biomass in the canyon and similar mass-specific respiration rates between the two habitats, it is not surprising that the macrofauna production and respiration were lower in the canyon than on the slope.

Despite the strong habitat effects, the benthic biomass, production, and size composition were not different across depth gradients, suggesting that the habitat difference (i.e., canyon and non-canyon) had greater impacts than the water depth. The individual regression analyses by transects also showed that the benthic production and respiration declined with depth only on the slope but not in the canyon, indicating that these bathymetric variations cannot be generalized across the habitats. Usually, the upper continental margin experiences the greatest depth-related environmental variations, resulting in ubiquitous bathymetric patterns in the benthic communities (Wei et al., 2010a; Wei et al., 2010b). Therefore, the non-depth-related patterns suggest that the high-energy conditions in the GPSC probably smoothed the typical strong bathymetric gradients in the deep-sea sediment.

This study shows that body-size composition can effectively detect the "canyon" effects in meiofauna and macrofauna communities, providing a useful alternative to taxonomical analyses. Since the same data have been analyzed based on taxon (Liao et al., 2017), polychaete family (Liao et al., 2017), nematode species (Liao et al., 2020), and body size compositions (this study), we can assess their "sensitivity" to the disturbed GPSC environment. To compare effect sizes, we calculated the ratio of the effect sum of squares ($SS_{habitat}$) divided by the total sum of squares (SS_{total}) in PERMANOVA (Fritz et al., 2012). The PERMANOVAs based on polychaete families (R^2 = 0.49) and nematode species (R^2 = 0.46) have the largest effect sizes (Table S3). The second highest is the analyses based on macrofauna (R^2 = 0.31) and meiofauna taxa (R^2 = 0.29). The smallest effect sizes are the analyses based on meiofauna (R^2 = 0.2) and macrofauna size compositions (R^2 = 0.12). Hence, while non-taxonomical analysis, such as body size composition, can detect significant habitat effects, they are generally less sensitive than taxonomical or species-level analysis.

The environmental drivers of the body size composition presented in this study are consistent with the previous studies based on taxon and nematode species compositions (Liao et al., 2017; Liao et al., 2020). We show that the meiofauna and macrofauna size compositions can be explained by factors related to internal-tide energy, food supply, temperature, and sediment characteristics. The canyon assemblages were primarily characterized by increasing internal tide energy (i.e., bottom current velocity, duration of sediment erosion, or low light transmission) and the slope assemblages by increasing food supplies (i.e., TOC or C/N ratio). The strong bottom currents may cause intermittent sediment resuspension and transports in the bottom nepheloid layer (Wang et al., 2008; Liu et al., 2010; Chiou et al., 2011). Also, the high internal tide energy can lead to long-lasting sediment winnowing to prevent the organic-rich particles from settling on the seafloor (Liao et al., 2017). Hence, the high-energy condition in the GPSC is a double-edged sword. On the one hand, the hydrodynamic regime erodes the sediment and causes long-term and recurrent disturbances in the local benthic communities. On the other hand, sediment resuspension and transport by the bottom-intensified currents decrease the total organic carbon (TOC) contents and, thus, the food supplies in the sediments.

5 Conclusions

Physical disturbance, food availability, temperature, and sediment characteristics controlled the biomass among size classes (or size bins) in benthic communities of the upper GPSC off SW Taiwan. The biomass-size compositions were distinctively different between the GPSC and adjacent slope. Typical "dome" patterns were observed in the normalized biomass size spectrum (NBSS), possibly due to a combination of factors, including the sampling artifact (i.e., sieve effects), physical disturbance, trophic cascade, food availability, and life-history traits. For the larger meiofauna (> 0.001 mg) and macrofauna (> 0.01 mg), the normalized biomass (or relative abundance) of the size bins decreased linearly with the mid-points of the size bins, in line with the linear normalized biomass size spectra (NBSS) observed elsewhere. These truncated NBSS slopes were steeper in the upper canyon than on the adjacent slope, suggesting that the largest meiofauna and macrofauna were relatively less abundant in the canyon. We hypothesized that the high-energy environment in the Gaoping Canyon (e.g., strong bottom currents and frequent turbidity flow) might have removed the larger-size individuals or favored the re-colonization of smaller individuals.

Nevertheless, the canyon meiofauna had a higher P/B ratio and respiration rate than the slope meiofauna, indicating that the canyon conditions favored the meiofauna with smaller body size and faster growth and metabolism. In contrast, the macrofauna communities in the canyon had a lower P/B ratio than the slope communities, possibly associated with disturbances in the canyon. Moreover, the community-level total biomass, secondary production, and respiration of meiofauna and macrofauna dropped significantly from the slope into the canyon habitats. These findings, along with previous studies (Liao et al., 2017; Liao et al., 2020), show that the energetic GPSC affected the total abundance, taxonomic composition, diversity, total biomass, growth, metabolism, and size composition of the local benthic communities. Understanding the effects of large-scale disturbance (e.g., internal tide and turbidity currents) on the benthic communities and the associated carbon cycling processes (e.g., body size, biomass, growth, and respiration) will enhance our ability to predict the impacts of climate changes in the submarine canyons ecosystems.

Data availability statement

The datasets presented in this study can be found in online repositories. The names of the repository/repositories and accession number(s) can be found below: https://github.com/chihlinwei/bbbs.

Author contributions

C-LW designed and conceived the study, to which all authors contributed ideas and discussion. J-XL and C-LW executed field sampling. J-XL conducted the laboratory work. C-CT, Y-TC, J-XL, and C-LW contributed to data analysis. C-CT, Y-TC, J-XL, and C-LW drafted the manuscript. All authors contributed to the interpretation of results and manuscript revisions. All authors contributed to the article and approved the submitted version.

Funding

This project is part of Fate of Terrestrial/Nonterrestrial Sediments in High Yield Particle-Export River-sea Systems (FATES-HYPERS), sponsored by the National Science and Technology Council (MOST 111-2611-M-002-021).

Acknowledgments

We thank the Institute of Oceanography (IO), the National Taiwan University (NTU), and the National Science and

Technology Council (NSTC) for supporting the fieldwork, analysis, and manuscript preparation. We thank Sen Jan and Ming-Da Chiou for providing the internal tide model. We thank Guan-Ming Chen and Yen-Li Liu for macrofauna body size measurements. We thank the captain, crew members, and technicians of the R/V Ocean Researcher I, as well as the graduate students who participated in the OCEAN 7090 Field Work in Marine Biology. Students collected the majority of samples and data through the field course.

Conflict of interest

The authors declare that the research was conducted in the absence of any commercial or financial relationships that could be construed as a potential conflict of interest.

Publisher's note

Supplementary material

The Supplementary Material for this article can be found online at: https://www.frontiersin.org/articles/10.3389/fmars.2023.1122143/full#supplementary-material

References

Aller, R. C. (1978). "The effects of animal-sediment interactions on geochemical processes near the sediment-water interface," in *Estuarine interactions* (Elsevier), 157–172. doi: 10.1016/B978-0-12-751850-3.50017-0

Andresen, H., and Brey, T. (2018) *BenthicPro: benthic energy flow*. Available at: https://github.com/HenrikeAndresen/BenthicPro.

Atkinson, A., Lilley, M. K. S., Hirst, A. G., McEvoy, A. J., Tarran, G. A., Widdicombe, C., et al. (2021). Increasing nutrient stress reduces the efficiency of energy transfer through planktonic size spectra. *Limnol. Oceanogr.* 66, 422–437. doi: 10.1002/lno.11613

Austen, M. C., and Widdicombe, S. (2006). Comparison of the response of meio-and macrobenthos to disturbance and organic enrichment. *J. Exp. Mar. Biol. Ecol.* 330, 96–104. doi: 10.1016/j.jembe.2005.12.019

Bett, B. J. (2013). Characteristic benthic size spectra: potential sampling artefacts. *Mar. Ecol. Prog. Ser.* 487, 1–6. doi: 10.3354/meps10441

Bett, B. J., van Reusel, A., Vincx, M., Soltwedel, T., Pfannkuche, O., Lambshead, P. J. D., et al. (1994). Sampler bias in the quantitative study of deep-sea meiobenthos. *Mar. Ecol. Prog. Ser.* 104, 197–203. doi: 10.3354/meps104197

Biles, C. L., Solan, M., Isaksson, I., Paterson, D. M., Emes, C., and Raffaelli, D. G. (2003). Flow modifies the effect of biodiversity on ecosystem functioning: an *in situ* study of estuarine sediments. *J. Exp. Mar. Biol. Ecol.* 285–286, 165–177. doi: 10.1016/S0022-0981(02)00525-7

Blanchard, J. L., Heneghan, R. F., Everett, J. D., Trebilco, R., and Richardson, A. J. (2017). From bacteria to whales: using functional size spectra to model marine ecosystems. *Trends Ecol. Evol.* 32, 174–186. doi: 10.1016/j.tree.2016.12.003

Boudreau, P., and Dickie, L. (1989). Biological model of fisheries production based on physiological and ecological scalings of body size. *Can. J. Fisheries Aquat. Sci.* 46, 614–623. doi: 10.1139/f89-078

Boudreau, P. R., Dickie, L. M., and Kerr, S. R. (1991). Body-size spectra of production and biomass as system-level indicators of ecological dynamics. *J. Theor. Biol.* 152, 329–339. doi: 10.1016/S0022-5193(05)80198-5

Brey, T. (1999). Growth performance and mortality in aquatic macrobenthic invertebrates. *Adv. Mar. Biol.* 35, 153–223. doi: 10.1016/S0065-2881(08)60005-X

Brey, T. (2012). A multi-parameter artificial neural network model to estimate macrobenthic invertebrate productivity and production. *Limnol. Oceanogr. Methods* 10, 581–589. doi: 10.4319/lom.2012.10.581

Brown, J. H., Gillooly, J. F., Allen, A. P., Savage, V. M., and West, G. B. (2004). Toward a metabolic theory of ecology. *Ecology* 85, 1771–1789. doi: 10.1890/03-9000

Chiang, C.-S., Hsiung, K.-H., Yu, H.-S., and Chen, S.-C. (2020). Three types of modern submarine canyons on the tectonically active continental margin offshore southwestern Taiwan. *Mar. Geophys Res.* 41, 4. doi: 10.1007/s11001-020-09403-z

Chiang, C.-S., and Yu, H.-S. (2022). Controls of submarine canyons connected to shore during the LGM sea-level rise: examples from Taiwan. *J. Mar. Sci. Eng.* 10, 494. doi: 10.3390/jmse10040494

Chiou, M.-D., Jan, S., Wang, J., Lien, R.-C., and Chien, H. (2011). Sources of baroclinic tidal energy in the gaoping submarine canyon off southwestern Taiwan. *J. Geophys. Res.* 116, C12016. doi: 10.1029/2011JC007366

Coull, B. C. (1990). Are members of the meiofauna food for higher trophic levels? *Trans. Am. Microscopical Soc.* 109, 233–246. doi: 10.2307/3226794

Danovaro, R. (2010). "Chapter 7 abundance of metazoan meiofauna," in *Methods for the study of deep-sea sediments, their functioning and biodiversity* (Boca Raton: CRC Press).

De Leo, F., Smith, C. R., Bowden, D. A., and Clark, M. R. (2010). Submarine canyons: hotspots of benthic biomass and productivity in the deep sea. *Proc. R. Soc. B.* 277, 2783–2792, rspb20100462. doi: 10.1098/rspb.2010.0462

Diaz, R. J., and Rosenberg, R. (1995). Marine benthic hypoxia: A review of its ecological effects and the behavioural responses of benthic macrofauna. *Oceanography Mar. Biol.: Annu. Rev.* 33, 245–303.

Diaz, R. J., and Rosenberg, R. (2001). Overview of anthropogenically-induced hypoxic effects on marine benthic fauna. In: *Coastal hypoxia: Consequences for living resources and ecosystems* (American Geophysical Union). doi: 10.1029/CE058p0129.

Dickie, L., Kerr, S., and Boudreau, P. (1987). Size-dependent processes underlying regularities in ecosystem structure. *Ecol. Monogr.* 57, 233–250. doi: 10.2307/2937082

Duplisea, D. E., Jennings, S., Warr, K. J., and Dinmore, T. A. (2002). A size-based model of the impacts of bottom trawling on benthic community structure. *Can. J. Fish. Aquat. Sci.* 59, 1785–1795. doi: 10.1139/f02-148

Duplisea, D. E., and Kerr, S. R. (1995). Application of a biomass size spectrum model to demersal fish data from the scotian shelf. *J. Theor. Biol.* 177, 263–269. doi: 10.1006/jtbi.1995.0243

Edwards, A. M., Robinson, J. P. W., Plank, M. J., Baum, J. K., and Blanchard, J. L. (2017). Testing and recommending methods for fitting size spectra to data. *Methods Ecol. Evol.* 8, 57–67. doi: 10.1111/2041-210X.12641

Elton, C. (1927). "The animal community," in *Animal ecology* (The Macmillan Company New York), 50–70.

Feller, R. J., and Warwick, R. M. (1988). "Energetics," in *Introduction to the study of meiofauna*. Eds. R. P. Higgins and H. Thiel (Washington, D.C: Smithsonian Institution Press), 181–196.

Fritz, C. O., Morris, P. E., and Richler, J. J. (2012). Effect size estimates: current use, calculations, and interpretation. *J. Exp. psychology: Gen.* 141, 2.

Gaedke, U. (1992). The size distribution of plankton biomass in a large lake and its seasonal variability. *Limnol. Oceanogr.* 37, 1202–1220. doi: 10.4319/lo.1992.37.6.1202

Gavey, R., Carter, L., Liu, J. T., Talling, P. J., Hsu, R., Pope, E., et al. (2017). Frequent sediment density flows during 2006 to 2015, triggered by competing seismic and weather events: Observations from subsea cable breaks off southern Taiwan. *Mar. Geol.* 384, 147–158. doi: 10.1016/j.margeo.2016.06.001

Giere, O. (2009). Meiobenthology: the microscopic motile fauna of aquatic sediments. *2nd* ed. Berlin: Springer. doi: 10.1007/978-3-540-68661-3

Górska, B., Soltwedel, T., Schewe, I., and Włodarska-Kowalczuk, M. (2020). Bathymetric trends in biomass size spectra, carbon demand, and production of Arctic benthos (76-5561 m, fram strait). *Prog. Oceanogr.* 186, 102370. doi: 10.1016/j.pocean.2020.102370

Górska, B., and Włodarska-Kowalczuk, M. (2017). Food and disturbance effects on Arctic benthic biomass and production size spectra. *Prog. Oceanogr.* 152, 50–61. doi: 10.1016/j.pocean.2017.02.005

Hargrave, B. T., and Thiel, H. (1983). Assessment of pollution-induced changes in benthic community structure. *Mar. Pollut. Bull.* 14, 41–46. doi: 10.1016/0025-326X(83)90189-3

Hsu, S.-K., Kuo, J., Lo, C.-L., Tsai, C.-H., Doo, W.-B., Ku, C.-Y., et al. (2008). Turbidity currents, submarine landslides and the 2006 pingtung earthquake off SW Taiwan. *Terrestrial Atmospheric Oceanic Sci.* 19, 767. doi: 10.3319/TAO.2008.19.6.767(PT

Iken, K., Brey, T., Wand, U., Voigt, J., and Junghans, P. (2001). Food web structure of the benthic community at the porcupine abyssal plain (NE atlantic): a stable isotope analysis. *Prog. Oceanogr.* 50, 383–405. doi: 10.1016/S0079-6611(01)00062-3

Jennings, S., Dinmore, T. A., Duplisea, D. E., Warr, K. J., and Lancaster, J. E. (2001). Trawling disturbance can modify benthic production processes. *J. Anim. Ecol.* 70, 459–475. doi: 10.1046/j.1365-2656.2001.00504.x

Jones, D. O. B., Yool, A., Wei, C.-L., Henson, S. A., Ruhl, H. A., Watson, R. A., et al. (2014). Global reductions in seafloor biomass in response to climate change. *Global Change Biol.* 20, 1861–1872. doi: 10.1111/gcb.12480

Jumars, P. A., Dorgan, K. M., and Lindsay, S. M. (2015). Diet of worms emended: An update of polychaete feeding guilds. *Annu. Rev. Mar. Sci.* 7, 497–520. doi: 10.1146/annurev-marine-010814-020007

Kleiber, M. (1932). Body size and metabolism. *Hilgardia* 6, 315–353. doi: 10.3733/hilg.v06n11p315

Klumpp, D. (1984). Nutritional ecology of the ascidian pyura stolonifera: Influence of body size, food quantity and quality on filter-feeding, respiration, assimilation efficiency and energy balance. *Mar. Ecol. Prog. series. Oldendorf* 19, 269–284. doi: 10.3354/meps019269

Kwong, L. E., and Pakhomov, E. A. (2021). Zooplankton size spectra and production assessed by two different nets in the subarctic northeast pacific. *J. Plankton Res.* 43, 527–545. doi: 10.1093/plankt/fbab039

Lee, I.-H., Wang, Y.-H., Liu, J. T., Chuang, W.-S., and Xu, J. (2009). Internal tidal currents in the gaoping (Kaoping) submarine canyon. *J. Mar. Syst.* 76, 397–404. doi: 10.1016/j.jmarsys.2007.12.011

Levin, L. A. (2003). Oxygen minimum zone benthos: adaptation and community response to hypoxia. *Oceanography Mar. Biology: Annu. Rev.* 41, 1:45.

Levin, L. A., and Sibuet, M. (2012). Understanding continental margin biodiversity: A new imperative. *Annu. Rev. Mar. Sci.* 4, 79–112. doi: 10.1146/annurev-marine-120709-142714

Liao, J.-X., Chen, G.-M., Chiou, M.-D., Jan, S., and Wei, C.-L. (2017). Internal tides affect benthic community structure in an energetic submarine canyon off SW Taiwan. *Deep Sea Res. Part I: Oceanographic Res. Papers* 125, 147–160. doi: 10.1016/j.dsr.2017.05.014

Liao, J.-X., Wei, C.-L., and Yasuhara, M. (2020). Species and functional diversity of deep-sea nematodes in a high energy submarine canyon. *Front. Mar. Sci.* 7. doi: 10.3389/fmars.2020.00591

Lin, B.-S., Brimblecombe, P., Lee, C.-L., and Liu, J. T. (2013). Tracing typhoon effects on particulate transport in a submarine canyon using polycyclic aromatic hydrocarbons. *Mar. Chem.* 157, 1–11. doi: 10.1016/j.marchem.2013.07.004

Lin, B.-S., Lee, C.-L., Brimblecombe, P., and Liu, J. T. (2016). Transport and fluxes of terrestrial polycyclic aromatic hydrocarbons in a small mountain river and submarine canyon system. *J. Environ. Manage.* 178, 30–41. doi: 10.1016/j.jenvman.2016.04.039

Liu, J. T., Hsu, R. T., Hung, J.-J., Chang, Y.-P., Wang, Y.-H., Rendle-Buhring, R., et al. (2016). From the highest to the deepest: the gaoping-River-Gaoping submarine canyon dispersal system. *Earth-Science Rev.* 274–300. doi: 10.1016/j.earscirev.2015.10.012

Liu, J. T., Wang, Y. H., Lee, I.-H., and Hsu, R. T. (2010). Quantifying tidal signatures of the benthic nepheloid layer in gaoping submarine canyon in southern Taiwan. *Mar. Geol.* 271, 119–130. doi: 10.1016/j.margeo.2010.01.016

Mazurkiewicz, M., Górska, B., Renaud, P. E., Legeżyńska, J., Berge, J., and Włodarska-Kowalczuk, M. (2019). Seasonal constancy (summer vs. winter) of benthic size spectra in an Arctic fjord. *Polar Biol.* 42, 1255–1270. doi: 10.1007/s00300-019-02515-2

Mazurkiewicz, M., Górska, B., Renaud, P. E., and Włodarska-Kowalczuk, M. (2020). Latitudinal consistency of biomass size spectra - benthic resilience despite environmental, taxonomic and functional trait variability. *Sci. Rep.* 10, 4164. doi: 10.1038/s41598-020-60889-4

Montagna, P. A., Baguley, J. G., Cooksey, C., Hartwell, I., Hyde, L. J., Hyland, J. L., et al. (2013). Deep-sea benthic footprint of the deepwater horizon blowout. *PloS One* 8, e70540. doi: 10.1371/journal.pone.0070540

Montagna, P. A., Baguley, J. G., Hsiang, C.-Y., and Reuscher, M. G. (2017). Comparison of sampling methods for deep-sea infauna. *Limnology Oceanography: Methods* 15, 166–183. doi: 10.1002/lom3.10150

Moyano, M., Illing, B., Christiansen, L., and Peck, M. A. (2017). Linking rates of metabolism and growth in marine fish larvae. *Mar. Biol.* 165, 5. doi: 10.1007/s00227-017-3252-4

Narayanaswamy, B. E., Bett, B. J., Lamont, P. A., Rowden, A. A., Bell, E. M., and Menot, L. (2016). "Corers and grabs," in *Biological sampling in the deep Sea* (Wiley-Blackwell). doi: 10.1002/9781118332535.ch10

Norkko, A., Villnäs, A., Norkko, J., Valanko, S., and Pilditch, C. (2013). Size matters: implications of the loss of large individuals for ecosystem function. *Sci. Rep.* 3, 2646. doi: 10.1038/srep02646

Ólafsson, E. (2003). Do macrofauna structure meiofauna assemblages in marine soft-bottoms? a review of experimental studies. *Vie Milieu / Life Environ.* 53, 249–265.

Parsons, T. (1969). The use of particle size spectra in determining the structure of a plankton community. *J. Oceanographical Soc. Japan* 25, 172–181. doi: 10.5928/kaiyou1942.25.172

Pepin, P. (1991). Effect of temperature and size on development, mortality, and survival rates of the pelagic early life history stages of marine fish. *Can. J. Fish. Aquat. Sci.* 48, 503–518. doi: 10.1139/f91-065

Petchey, O. L., and Belgrano, A. (2010). Body-size distributions and size-spectra: universal indicators of ecological status? *Biol. Lett.* doi: 10.1098/rsbl.2010.0240

Peters, R. H. (1983). *The ecological implications of body size* (Cambridge: Cambridge University Press). doi: 10.1017/CBO9780511608551

Platt, T. (1985). "Structure of marine ecosystems: its allometric basis," in *Ecosystem theory for biological oceanography*., eds. R. E. Ulanowicz and T. Platt. Canadian Bulletin of Fisheries and Aquatic Sciences 213, 55–64.

Qu, F., Nunnally, C., Rowe, G. T., Qu, F., Nunnally, C., and Rowe, G. T. (2015). Polychaete annelid biomass size spectra: the effects of hypoxia stress. *J. Mar. Biology J. Mar. Biol.* 2015, e983521. doi: 10.1155/2015/983521

Queirós, A. M., Hiddink, J. G., Kaiser, M. J., and Hinz, H. (2006). Effects of chronic bottom trawling disturbance on benthic biomass, production and size spectra in different habitats. *J. Exp. Mar. Biol. Ecol.* 335, 91–103. doi: 10.1016/j.jembe.2006.03.001

Quiroga, E., Gerdes, D., Montiel, A., Knust, R., and Jacob, U. (2014). Normalized biomass size spectra in high Antarctic macrobenthic communities: linking trophic position and body size. *Mar. Ecol. Prog. Ser.* 506, 99–113. doi: 10.3354/meps10807

Quiroga, E., Quiñones, R., Palma, M., Sellanes, J., Gallardo, V. A., Gerdes, D., et al. (2005). Biomass size-spectra of macrobenthic communities in the oxygen minimum zone off Chile. *Estuarine Coast. Shelf Sci.* 62, 217–231. doi: 10.1016/j.ecss.2004.08.020

Rachor, E. (1975). Quantitative untersuchungen über meiobenthos der nordostatlantischen tiefsee. *"Meteor" ForschErgebn (Ser. D)* 21, 1–10.

R Core Team (2022). *R: a language and environment for statistical computing* (Vienna, Austria: R Foundation for Statistical Computing). Available at: http://www.R-project.org/.

Rossberg, A. G., Gaedke, U., and Kratina, P. (2019). Dome patterns in pelagic size spectra reveal strong trophic cascades. *Nat. Commun.* 10, 4396. doi: 10.1038/s41467-019-12289-0

Ruxton, G. D., and Houston, D. C. (2004). Energetic feasibility of an obligate marine scavenger. *Mar. Ecol. Prog. Ser.* 266, 59–63. doi: 10.3354/meps266059

Saiz-Salinas, J. I., and González-Oreja, J. A. (2000). Stress in estuarine communities: Lessons from the highly-impacted bilbao estuary (Spain). *J. Aquat. Ecosystem Stress Recovery* 7, 43–55. doi: 10.1023/A:1009919429985

Saiz-Salinas, J., and Ramos, A. (1999). Biomass size-spectra of macrobenthic assemblages along water depth in Antarctica. *Mar. Ecol. Prog. Ser.* 178, 221–227. doi: 10.3354/meps178221

Schewe, I., and Soltwedel, T. (1999). Deep-sea meiobenthos of the central Arctic ocean: distribution patterns and size-structure under extreme oligotrophic conditions. *Vie Milieu/Life Environ.* 49, 79–92.

Schratzberger, M., and Ingels, J. (2018). Meiofauna matters: The roles of meiofauna in benthic ecosystems. *J. Exp. Mar. Biol. Ecol.* 502, 12–25. doi: 10.1016/j.jembe.2017.01.007

Schwinghamer, P. (1981). Characteristic size distributions of integral benthic communities. *Can. J. Fish. Aquat. Sci.* 38, 1255–1263. doi: 10.1139/f81-167

Schwinghamer, P. (1988). Influence of pollution along a natural gradient and in a mesocosm experiment on biomass-size spectra of benthic communities. *Mar. Ecol. Prog. Ser.* 46, 199–206. doi: 10.3354/meps046199

Schwinghamer, P., Hargrave, B. T., Peer, D., and Hawkins, C. (1986). Partitioning of production and respiration among size groups of organisms in an intertidal benthic community. *Mar. Ecol. Progr Ser.* 31, 131–142. doi: 10.3354/meps031131

Sheldon, R., Prakash, A., and Sutcliffe, (1972). The size distribution of particles in the ocean. *Limnol. Oceanogr.* 17, 327–340. doi: 10.4319/lo.1972.17.3.0327

Shin, Y. J., Rochet, M. J., Jennings, S., Field, J. G., and Gislason, H. (2005). Using size-based indicators to evaluate the ecosystem effects of fishing. *ICES J. Mar. Sci.* 62, 384–396. doi: 10.1016/j.icesjms.2005.01

Shurin, J. B., Gruner, D. S., and Hillebrand, H. (2006). All wet or dried up? real differences between aquatic and terrestrial food webs. *Proc. R. Soc. B: Biol. Sci.* 273, 1–9. doi: 10.1098/rspb.2005.3377

Solan, M., Cardinale, B. J., Downing, A. L., Engelhardt, K. A. M., Ruesink, J. L., and Srivastava, D. S. (2004). Extinction and ecosystem function in the marine benthos. *Science* 306, 1177–1180. doi: 10.1126/science.1103960

Soltwedel, T., Pfannkuche, O., and Thiel, H. (1996). The size structure of deep-sea meiobenthos in the north-eastern Atlantic: nematode size spectra in relation to environmental variables. *J. Mar. Biol. Assoc. United Kingdom* 76, 327–344. doi: 10.1017/S0025315400030587

Sommer, U., Meusel, B., and Stielau, C. (1999). An experimental analysis of the importance of body-size in the seastar-mussel predator-prey relationship. *Acta Oecologica* 20, 81–86. doi: 10.1016/S1146-609X(99)80019-8

Sprules, W., and Bowerman, J. (1988). Omnivory and food chain length in zooplankton food webs. *Ecology* 69, 418–426. doi: 10.2307/1940440

Sprules, W. G., Brandt, S., Stewart, D., Munawar, M., Jin, E., and Love, J. (1991). Biomass size spectrum of the lake Michigan pelagic food web. *Can. J. Fisheries Aquat. Sci.* 48, 105–115. doi: 10.1139/f91-015

Sprules, W. G., Casselman, J., and Shuter, B. (1983). Size distribution of pelagic particles in lakes. *Can. J. Fisheries Aquat. Sci.* 40, 1761–1769. doi: 10.1139/f83-205

Su, C.-C., Tseng, J.-Y., Hsu, H.-H., Chiang, C.-S., Yu, H.-S., Lin, S., et al. (2012). Records of submarine natural hazards off SW Taiwan. *Geological Society London Special Publications* 361, 41–60. doi: 10.1144/SP361.5

Sukhotin, A. A., Abele, D., and Pörtner, H.-O. (2002). Growth, metabolism and lipid peroxidation in mytilus edulis: age and size effects. *Mar. Ecol. Prog. Ser.* 226, 223–234. doi: 10.3354/meps226223

Thompson, G. A., Dinofrio, E. O., and Alder, V. A. (2013). Structure, abundance and biomass size spectra of copepods and other zooplankton communities in upper waters of the southwestern Atlantic ocean during summer. *J. Plankton Res.* 35, 610–629. doi: 10.1093/plankt/fbt014

Vetter, E. W., and Dayton, P. K. (1998). Macrofaunal communities within and adjacent to a detritus-rich submarine canyon system. *Deep Sea Res. Part II: Topical Stud. Oceanography* 45, 25–54. doi: 10.1016/S0967-0645(97)00048-9

Vetter, E. W., and Dayton, P. K. (1999). Organic enrichment by macrophyte detritus, and abundance patterns of megafaunal populations in submarine canyons. *Mar. Ecol. Prog. Ser.* 186, 137–148. doi: 10.3354/meps186137

Volkenborn, N., Meile, C., Polerecky, L., Pilditch, C. A., Norkko, A., Norkko, J., et al. (2012). Intermittent bioirrigation and oxygen dynamics in permeable sediments: An experimental and modeling study of three tellinid bivalves. *J. Mar. Res.* 70, 794–823. doi: 10.1357/002224012806770955

Vranken, G., and Heip, C. (1986). The productivity of marine nematodes. *Ophelia* 26, 429–442. doi: 10.1080/00785326.1986.10422004

Wang, Y. H., Lee, I. H., and Liu, J. T. (2008). Observation of internal tidal currents in the kaoping canyon off southwestern Taiwan. *Estuarine Coast. Shelf Sci.* 80, 153–160. doi: 10.1016/j.ecss.2008.07.016

Warwick, R. M. (2014). Meiobenthos and macrobenthos are discrete entities and not artefacts of sampling a size continuum: Comment on bett, (2013). *Mar. Ecol. Prog. Ser.* 505, 295–298. doi: 10.3354/meps10830

Warwick, R. M., and Clarke, K. R. (1984). Species size distributions in marine benthic communities. *Oecologia* 61, 32–41. doi: 10.1007/BF00379085

Warwick, R. M., and Gee, J. M. (1984). Community structure of estuarine meiobenthos. *Mar. Ecol. Prog. Ser.* 18, 97–111. doi: 10.3354/meps018097

Wei, C.-L., Rowe, G. T., Escobar-Briones, E., Boetius, A., Soltwedel, T., Caley, M. J., et al. (2010a). Global patterns and predictions of seafloor biomass using random forests. *PloS One* 5, e15323. doi: 10.1371/journal.pone.0015323

Wei, C.-L., Rowe, G. T., Escobar-Briones, E., Nunnally, C., Soliman, Y., and Ellis, N. (2012). Standing stocks and body size of deep-sea macrofauna: predicting the baseline of 2010 deepwater horizon oil spill in the northern gulf of Mexico. *Deep Sea Res. Part I: Oceanographic Res. Papers* 69, 82–99. doi: 10.1016/j.dsr.2012.07.008

Wei, C.-L., Rowe, G. T., Hubbard, G. F., Scheltema, A. H., Wilson, G. D. F., Petrescu, I., et al. (2010b). Bathymetric zonation of deep-sea macrofauna in relation to export of surface phytoplankton production. *Mar. Ecol. Prog. Ser.* 399, 1–14. doi: 10.3354/meps08388

Wilson, S. K., Fisher, R., Pratchett, M. S., Graham, N., Dulvy, N. K., Turner, R. A., et al. (2010). Habitat degradation and fishing effects on the size structure of coral reef fish communities. *Ecol. Appl.* 20, 442–451. doi: 10.1890/08-2205.1

Wrede, A., Andresen, H., Asmus, R., Wiltshire, K. H., and Brey, T. (2019). Macrofaunal irrigation traits enhance predictability of nutrient fluxes across the sediment-water interface. *Mar. Ecol. Prog. Ser.* 632, 27–42. doi: 10.3354/meps13165

Yurista, P. M., Yule, D. L., Balge, M., VanAlstine, J. D., Thompson, J. A., Gamble, A. E., et al. (2014). A new look at the lake superior biomass size spectrum. *Can. J. Fish. Aquat. Sci.* 71, 1324–1333. doi: 10.1139/cjfas-2013-0596